

9T
571
2340.
233

12T

THERMAL PRECIPITATION AND AEROSOL SAMPLING

A THESIS

Presented to
the Faculty of the Graduate Division
Georgia Institute of Technology

In Partial Fulfillment
of the Requirements for the Degree
Master of Science in the School of Chemical Engineering

by
Mendel Temkin Gordon

June 1954

571

THERMAL PRECIPITATION AND AEROSOL SAMPLING

Approved:

[Handwritten signature]

Date Approved by Chairman: June 2, 1954

PREFACE

During the last eighty-four years, a score or more of papers and articles have appeared on the theoretical and practical aspects of thermal repulsion. However, the state of the art, where filters and collectors utilizing this force are concerned, has not progressed far beyond Aitken's heated wire of 1884. Authorities in the aerosol field are all in agreement that thermal precipitators may be made 100 per cent efficient. It would certainly appear that, through the application of imagination and ingenuity, a device utilizing thermal repulsion could be constructed which would offer man a means to protect himself from his environment polluted now by automobiles and industry, and likely to be polluted in the future by atom and cobalt bombs.

The author wishes to express his gratitude to Professor J. M. Dalla Valle for his introduction to the fascinating field of "Micromeritics," and to Professor T. W. Kethley, whose advice and encouragement were invaluable. In addition, the author wishes to acknowledge the helpful suggestions of Professor Clyde Orr, Jr., which led to the design of the Thermal Precipitator, Model I, and to thank him for his careful editing of the manuscript.

TABLE OF CONTENTS

	Page
PREFACE	ii
LIST OF TABLES	v
LIST OF FIGURES	vi
ABSTRACT	vii
CHAPTER	
I. INTRODUCTION	1
Objectives	2
Literature Review	2
II. EXPERIMENTAL METHODS	11
Thermal Precipitator, Model I	11
Thermal Precipitator, Model II	16
III. DISCUSSION OF RESULTS	27
Previous Mathematical Analyses of Thermal Precipitation	27
Mathematical Analysis of Areal-Type Thermal Precipitators	35
IV. CONCLUSIONS	59
V. RECOMMENDATIONS	61
APPENDIX	62
Sample Calculations	63
Derivations	66
Calculation of Spacing	68

	Page
Assembly and Operating Instructions for Thermal Precipitators, Models II and IIa	69
Symbols	70
BIBLIOGRAPHY	73

LIST OF TABLES

Table	Page
1. Results Obtained with Thermal Precipitator, Model I, and Magnesium Oxide Aerosols	15
2. Results Obtained with Thermal Precipitator, Model II, and Magnesium Oxide Aerosols	20
3. Physical Properties of Aerosol Materials	21
4. Results Obtained with Thermal Precipitator, Model IIA, and Magnesium Oxide Aerosols	22
5. Results Obtained with Thermal Precipitator, Model IIA, and Diethylene Glycol Aerosols	24
6. Results Obtained with Thermal Precipitator, Model IIA, and Mineral Oil Aerosols	25
7. Results Obtained with Thermal Precipitator, Model IIA, and <u>Serratia marcescens</u> Bacterial Aerosols	26
8. Calculated Results with Thermal Precipitator, Model I, and Magnesium Oxide Aerosols	41
9. Calculated Results with Thermal Precipitator, Model II, and Magnesium Oxide Aerosols	42
10. Calculated Results with Thermal Precipitator, Model IIA, and Magnesium Oxide Aerosols	43
11. Calculated Results with Thermal Precipitator, Model IIA, and Diethylene Glycol Aerosols	45
12. Calculated Results with Thermal Precipitator, Model IIA, and Mineral Oil Aerosols	46
13. Calculated Results with Thermal Precipitator, Model IIA, and <u>Serratia marcescens</u> Bacterial Aerosols	47
14. Experimental and Calculated Data from Harrington and Crozier (14)	65

LIST OF FIGURES

Figure	Page
1. Cross Sectional Diagram of the Hot Plate of Thermal Precipitator, Model I	13
2. Thermal Precipitator, Model II	17
3. The Components of Thermal Precipitator, Model II	18
4. Diagrammatic Sketch of Thermal Precipitator, Model IIa	38
5. Results with Thermal Precipitator, Model I, and Magnesium Oxide Aerosols	48
6. Results with Thermal Precipitator, Model II, and Magnesium Oxide Aerosols	49
7. Results with Thermal Precipitator, Model IIa, and Magnesium Oxide Aerosols	50
8. Results with Thermal Precipitator, Model IIa, and Diethylene Glycol Aerosols	51
9. Results with Thermal Precipitator, Model IIa, and Mineral Oil Aerosols	52
10. Results with Thermal Precipitator, Model IIa, and <u>Serratia marcescens</u> Bacterial Aerosols	53
11. Results of Harrington and Crozier (14)	57
12. The Terminal Settling Velocity of Water Droplets in Thermal and Gravitational Fields	58

ABSTRACT

The object of this investigation was to design and construct a thermal precipitator which could be used routinely to sample aerosols ranging from crystalline smokes to airborne viable organisms, such as spores and bacteria. It was intended, also, to correlate the operating variables in such a manner that the performance of areal thermal precipitators could be predicted.

Air sampling devices of extended area, based on the principle of thermal repulsion, have been designed and constructed for the purpose of efficiently collecting airborne particles at rates considerably in excess of those used in previous samplers utilizing the same force. In the apparatus described herein, air containing the suspended matter is made to flow radially between two parallel circular surfaces which are maintained at different temperatures. The suspended matter in the air sample is precipitated upon the colder of the two surfaces in the form of an annular area the width of which depends upon the temperature gradient between the two surfaces, the rates at which the air is drawn through the apparatus, and the physical properties of the suspended material.

Equations have been derived which permit the calculation of the terminal velocities of aerosol particles being acted on by gravitational and thermal forces in devices having various geometric configurations. When these forces are acting in the same direction, the terminal velocity

of the particle may be expressed by the equation

$$v = \frac{D_p^2 C_m \rho_p g}{18\mu} + \frac{3}{2} C_m \frac{R\mu}{MP} \frac{k}{2k + k_p} \frac{\Delta T}{x},$$

where C_m = Cunningham's correction factor to Stokes' Law = $1 + \frac{2A\lambda}{D_p}$,

D_p = particle diameter,

g = acceleration of gravity,

k = gas thermal conductivity,

k_p = particle thermal conductivity,

M = molecular weight of gas,

P = absolute pressure,

R = gas constant,

ΔT = temperature difference,

v = particle terminal velocity,

x = distance between hot and cold surface,

μ = gas viscosity,

ρ_p = density of particle.

When forces act in opposition, the sign of one of the terms in the equation becomes minus.

Methods are described by which the operating characteristics of any areal type thermal precipitator can be predicted. Expressions are presented for the terminal velocities of particles collected in the thermal precipitators described herein, in terms of the volume rate of flow of the sample, the deposit length and the inlet radius. Experimental results and values obtained from these equations have been found to be

in agreement. Furthermore, apparatus designed on the basis of the relations given are being successfully used in a number of laboratories.

It is suggested that the use of thermal precipitation to separate different species of airborne particles on the basis of differences in thermal conductivity would be practical.

CHAPTER I

INTRODUCTION

Just as weight is the force associated with a gravitational field, so thermal repulsion is the force associated with a thermal field. Since few circumstances of thermal equilibrium exist, results of this force can be observed with little difficulty. The precipitation of dust and smoke from warm gases on cool surfaces is a common example of thermal repulsion. The black streaks which are observed on the walls above radiators and hot air registers are caused by thermal repulsion, for instance. Although various manifestations of thermal repulsion have been observed and documented since its first discovery over eighty years ago, it was not until very recently that researchers were able to measure the magnitude of this force, to determine the variables affecting it, and to postulate a relationship for this repulsion in terms of these variables.

In general, most of the investigations of thermal repulsion have been done by those interested in aerosols, i.e., finely divided matter suspended in gases. Early investigators perceived that an aerosol sampler or filter utilizing thermal repulsion would have an efficiency of 100 per cent and, accordingly, designed and built several types of apparatus based on this principle. These precipitators and filters were applications of observed phenomena and were not appreciable improvements on the classical designs.

Objectives.--At the Engineering Experiment Station of the Georgia Institute of Technology, a considerable interest was developed in a sampling device utilizing thermal repulsion for use on a project dealing with bacterial aerosols. Conditions to be met by a satisfactory sampler for this project were:

1. The environment in the sampler should be favorable to the survival of the bacteria.
2. The collection of the bacteria should be accomplished in such a manner which would allow subsequent removal and culture.
3. The sampling rate should be appreciably larger than existing thermal precipitation devices.

This interest has been broadened to include the fundamental relationships involved in the mechanism of the operation of thermal precipitators.

Literature Review.--With the above in mind, a review of the literature on thermal repulsion, thermal precipitators, thermal filters, and radiometers was undertaken. That a dust free space surrounds a heated wire suspended in a dusty gas was first recorded by Tyndall (24) in a paper presented in 1870. Tyndall concluded that, when the wire was at white heat, the dust free space was caused by the incineration of the particles and that, at lower temperatures, the effect was due to a redistribution of the suspended particles caused by a density decrease of the heated air without an accompanying density decrease of the particles.

In 1876, Osborne Reynolds (21) performed experiments which

indicated that the operation of a vane-type radiometer was dependent on the presence of a small amount of gas in the radiometer bulb. A radiometer is a partially evacuated bulb with a pivoted rotating element of four vanes. Each vane has one side polished and the other blackened. When exposed to light or heat, the element rotates. From his experiments, Reynolds concluded that thermal repulsion is the motivating force of the radiometer.

William Crookes (7), in 1879, presented a paper before the Royal Society (London) which described the measurement of the radiometer effect as a function of total gas pressure in the bulb, geometry of the vanes, temperature of the bulb, and intensity of incident light. From the result of these experiments, Crookes confirmed the fact that the action of the radiometer was due to the reaction of the heated residual gas molecules against the vanes. Crookes also performed several experiments in which he attempted to measure directly the radiometer force as a function of air pressure and heat intensity. His apparatus consisted of a heat source and a torsion balance made from a small clear mica disk attached to a quartz fiber. The disk and fiber were surrounded by a glass envelope in which the gas pressure could be varied. In this apparatus the radiometer force was found to be a maximum at an absolute pressure of 4×10^{-7} atmospheres.

Probably the first characterization of the dust-free space as a "dark-plane" was made by Lord Rayleigh (20) in a paper presented in 1882. After reviewing Tyndall's work and quoting a Professor Frankland as stating that Tyndall's experiments prove that "a very large proportion

of the suspended particles in the London atmosphere consists of water and other volatile liquid or solid matter," Rayleigh describes his own experiments and conclusions. For his experimental work, Rayleigh built a small chamber (about the size of a cigar box) with three sides made of glass. One of these sides was for observation and could be removed for the introduction of smokes from smoldering brown paper. A copper rod, whose end had been hammered into a 1/4 inch wide blade, was then inserted into the box through the side opposite that used for observation. The externally projecting end of the rod was then heated with an alcohol lamp and a beam of sunlight directed on the rod within the chamber. Writes Rayleigh,

At a moderate distance above the blade it (i.e., the dark plane) is narrow, sometimes so narrow as almost to render necessary a magnifying glass, but below, where it attaches itself to the blade, it widens out to the full width. . . . Whether the heated body be a thin blade or a cylindrical rod, the fluid passes round the obstacle according to the electrical law of flow, the stream-lines in the rear of the obstacle being of the same form as in front of it. This peculiarity of behaviour is due to the origin of motion being at the obstacle itself, especially at its hinder surface. If a stream be formed by other means, and impinge upon the same obstacle without a difference of temperature, the motion is of a different character altogether and eddies are formed in the shadow.

Rayleigh heated a 1/4 inch diameter glass rod, inserted it into the box and observed the decrease in size of the dark plane as the rod cooled. While the dark plane was still distinct, the rod was taken out and it was found to be only slightly warm to the touch. As Rayleigh states, "It was almost impossible to believe the smoky matter had been evaporated."

When Rayleigh placed a glass rod, cooled in a salt-ice-water

mixture, in the box, the dark plane was observed to extend downward. To quote Rayleigh, "This result not merely shows that the dark plane is not due to evaporation, but also excludes any explanation depending upon an augmentation in the difference of densities of fluid and foreign matter." On the evidence of the foregoing experiments, Rayleigh attempted several explanations of the dark plane; however, he ends the paper with the statement that, "no absolute conclusion can be drawn."

J. Aitken (1) was the next investigator to report on thermal repulsion. His main interest in the phenomenon was its effect on preventing the deposition of dust on the internal surfaces of the lungs. He established that a warm moist surface has a greater thermal repulsion effect than a warm dry one. Aitken also made some preliminary experiments with a thermal precipitator consisting of a horizontal, heated wire placed between two vertical glass plates. When the warm aerosol flowed upwards past the wire, dust particles were found to be deposited on the plates.

By means of a box similar to that used by Rayleigh, Aitken followed the action of individual particles in the presence of a thermal field and established definitely that there was a repulsion of solid airborne particles by a heated surface.

A thermal filter constructed by Aitken consisted of two concentrically mounted tubes. In this apparatus, the aerosol flowed between the inner and outer tube, the outer tube being heated by a gas flame or steam. With this filter he determined that the precipitation of particles was complete at proper flows and thermal gradients. His

examination of the filter efflux led him to conclude, "the filter was doing its work thoroughly, not a single particle . . . not even one of the very minute and invisible ones . . . escaping it."

Aitken performed many different types of experiments involving these phenomena. One of these experiments he describes as follows:

This repulsion (i.e., thermal) may be illustrated by placing a hot and cold surface together. A piece of cold glass, for instance, slides about in a remarkably easy way on a hot surface of glass.

The explanation given by Aitken for the mechanism of thermal repulsion was that there is a bombardment of the particle by a greater number of higher energy gas molecules from the direction closest to the heated surface.

In 1910, Knudsen (17) developed the theory for the mechanism of thermal repulsion when the particle radius is less than twice the mean free path of the gas molecules, i.e., at very low pressures. From this theory stemmed the final explanation of the mechanism of thermal repulsion.

W. D. Bancroft (2), in 1920, in an article reviewing work done by United States Army Chemical Warfare Service personnel, described the mechanism of thermal force postulated by Maxwell (18). The thermal force was described as being due to a combination of molecular bombardment and creep of fluid around the particle. Or in Bancroft's words,

Around each particle of dust there is a film of absorbed air. If each particle is heated on one side, this film will be diminished, but air will flow around the particle from the cooler to the warmer side tending to restore the equilibrium. This will cause a movement of the particle towards the cooler portions of the space. This means that the dust particle is sucked toward the cooler zone while Aitken considers that it is driven from

the hotter one. Actually, both things are taking place simultaneously.

In the experiments described by Bancroft, a thermal filter of the type of Aitken was employed, except in this case the inner surface of the annulus was heated and the outer one cooled. Tobacco smoke was used for the test. For one such filter thirty inches long, no particles were visible in the effluent for a temperature difference of 80° F and a flow rate of 550 cc./min. A similar filter twelve inches long under the conditions of 80° F and 195 cc./min. also gave no visible smoke in the effluent.

The relationship between temperature gradient and flow rate, for constant tube length, are practically linear according to Bancroft. He concluded, however, that the military application of the filter is impractical due to the low flow rates and the high power consumption.

The mechanism of motion for the vane radiometer was first approximated by an equation derived by A. Einstein (10) in 1924. This equation stated that the thermal force is proportional to the absolute pressure, the temperature gradient and a linear dimension of the vane.

Various other physicists developed the formulas further until P. Epstein (11) postulated a final equation describing the force of thermal repulsion in terms of the thermal and physical properties of the body and the gas. The mechanism was then described as a process of thermal creep with the bombardment of the molecules serving only to supply heat.

In 1936, in a symposium dealing with dust problems, W. Cawood (6) re-emphasized that the dark plane surrounding hot bodies is caused by

thermal gradients and not by radiation pressure. He further postulated an equation for calculating the velocity of the particle on the assumption that the motion of a suspended particle was due to the higher energy of the gas molecules striking it from the direction of the heated surface.

Another paper in the same symposium dealt with experiments using a chamber similar to that of Rayleigh. H. H. Watson (25), author of that paper, measured the width of the dark space as a function of the temperature difference between the hot body and the ambient air, the geometry of the hot body and the total pressure in the chamber. Watson reported that the magnitude of the dark space was independent of the nature of the dust and of the particle size. These experiments resulted in an equation relating the thickness of the dark space with the thermal gradient and the unit heat loss of the hot body. Watson also presented the design of a practical hot wire thermal precipitator, based on an idea of Aitken.

In 1939, S. C. Blacktin (4) postulated a theory of lattice repulsion where a heated cavity takes the place of a heated object in repelling particles. He designed and patented a filter in which dust-laden air or flue gas is drawn through a heated gauze. The dust particles are prevented from penetrating the heated gauze by lattice repulsion.

In conjunction with their research into the general properties of aerosols, Rosenblatt and Lamer (22) investigated the effects of a thermal gradient. They measured the repulsion velocity of single droplets at various gradients and pressures. This velocity was confirmed

to be independent of particle size, directly proportional to thermal gradient and inversely proportional to pressure.

A departure from the classical designs of Aitken was made by Harrington and Crozier (14). Their apparatus consisted of two parallel plates. The lower plate was heated and the upper plate cooled, with the aerosol being drawn between the plates. At very high temperature gradients, they were able to use flow rates as high as one liter/minute. However, difficulties in maintaining uniform temperatures over the two surfaces resulted in non uniform deposits which prevented the full utilization of the increased capacity.

In 1951, Bredl and Grieve (5) described a thermal precipitator developed by them for use in the determination of the suspended matter in flue gases. In general, it resembled the filter described by Bancroft, however, instead of the central tube being a cylinder, it was an electrically heated cone frustrum. Thus the cross sectional area of the sampler and likewise the distance between the surfaces decreased with distance from the inlet. This last, they explained, caused the larger particles to be deposited near the entrance, and the smaller near the exit. Since the fly ash particles are usually larger than the carbon particles in flue gases, this classifying effect made the relative amounts of ash and carbon determinable.

Finally, in August of 1952, R. L. Saxton and W. E. Ranz (23) published a highly significant paper in which they described the actual measurement of the thermal force on an aerosol particle. These experiments substantiated the theories and derivations of Epstein (11). The

method of measuring thermal force is quite interesting as it is an adaptation of Millikan's familiar oil-drop experiment. As Saxton and Ranz describe it,

For each particle, the times of free fall and of rise under a known electrostatic field were recorded so that the mass and charge could be computed. Then a temperature gradient was established in the air between the plates, the upper plate being made the hotter so as to insure the absence of convection. The strength of the electrostatic field needed to lift the particle against the temperature gradient was determined and the thermal force was obtained as the difference between this electrical force and the sum of gravity and drag forces.

The results of these experiments were used by Saxton and Ranz to test the validity of the various equations which have been postulated. The deviation of the measured force from that predicted by equations of Cawood, Einstein, and Epstein was found to be 249, 68.5 and 5.4 per cent respectively.

The author (12, 13, and 16) has participated in the publication of several articles on various applications of thermal precipitation.

CHAPTER II

EXPERIMENTAL METHODS

The thermal precipitators used for this investigation were constructed in the machine shop of the Engineering Experiment Station under the supervision of the author. Laboratory apparatus such as flow-meters, pumps, chemicals, variable transformers, etc. were available in the Bioengineering Laboratory of the Engineering Experiment Station where the author was employed part-time. Special apparatus and materials were supplied by the National Institutes of Health project dealing with bacterial aerosols which had an interest in the results of this thesis.

The thermal precipitators built are of the extended area type. A limitation of the first design was that it had to be placed within an enclosure through which the aerosol was drawn or forced. In both cases the aerosol was drawn between two parallel circular plates.

Thermal Precipitator, Model I.--The first sampler built was made to deposit airborne bacteria directly onto an agar surface in a Petri dish. This device consisted essentially of a brass plate three inches in diameter. A one-half inch diameter hole in the center served as an opening through which air could be drawn. The bottom of the plate had a flat portion one and one-quarter inches in diameter in the center and then was tapered to the outer circumference. The outer edge of this surface was 0.020 inch higher than the flat portion. The upper part of the

plate had a recess in which resistance wire, imbedded in an insulating cement, was placed. The entire plate was attached to a machined piece of temperature-resistant plastic which, in turn, was fitted to a one-half inch diameter brass tube, one foot long. A diagram of this device appears in Figure 1. The temperature of the brass plate was regulated by varying the voltage applied across the resistance wire. This assembly was mounted on a Penetrometer Stand in such a fashion that the bottom of the brass plate, or heated surface, could be accurately positioned a very small distance above the surface of the agar in a Petri dish.

To use this device, it was necessary to place the entire apparatus in a chamber within which an aerosol could be established. A plastic box, two feet on a side, was used for this purpose. This device was found to melt the agar in the Petri dish, thus indicating a surface temperature sufficiently high to injure the deposited bacteria. Since it was not considered feasible to provide a means of keeping the surface of the agar below its melting point, it was decided to abandon the use of agar as a collecting surface.

The hot plate assembly was modified by extending four of the eight screws used to fasten the brass plate to the plastic holder. The entire assembly then rested on the pointed ends of these four screws. The distance the screws extended from the plate could be adjusted so that the flat section of this plate was a very small distance from, and parallel to, the supporting surface. A hollow disk through which cooling water could be passed was made. This disk was two inches high and three inches in diameter. This now became the supporting surface.

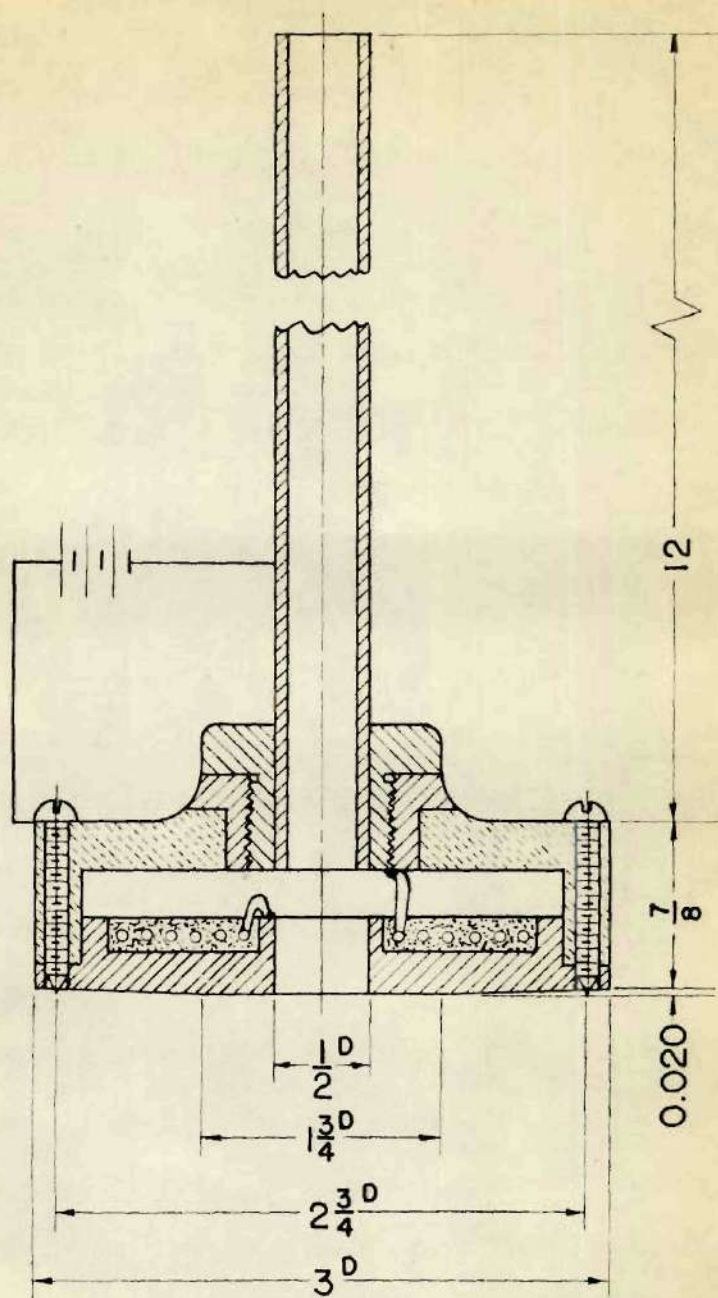


Figure 1. Cross Sectional Diagram of the Hot Plate of Thermal Precipitator, Model I.

A thin glass plate, one-sixteenth inch thick and four inches square was used as a surface upon which to deposit the particulate matter of an aerosol. It was found that this glass plate was too thick to permit obtaining sufficiently high thermal gradients. Therefore, thin glass disks, 0.008 inch thick and three inches in diameter, obtained from C. A. Hausser and Son, Philadelphia, Pennsylvania were used.

The precipitator was installed in the plastic chamber mentioned above, in which holes had been drilled for the required utilities such as water, electricity, and vacuum. Vacuum for use in drawing the aerosol into the precipitator was obtained by using a compressed air ejector. The flow of sampling air was controlled with a needle valve and metered with a calibrated orifice meter or a small wet-test meter. Thermocouples were imbedded in the hot and cold surfaces to measure their temperatures.

A magnesium oxide aerosol was found to be suitable for testing the precipitator. This magnesium oxide aerosol was generated by burning a short length (one to two inches) of magnesium ribbon in the chamber. This aerosol was aged for thirty to forty-five minutes in order to allow the largest particles to settle. During this time the thermal gradient in the precipitator was maintained. After the aerosol had aged sufficiently, a sample was taken with the precipitator at a constant flow rate. After a short time, determined by experiment, the chamber was opened, the sampler disassembled, and the dimensions of the deposit of magnesium oxide measured and recorded. Table 1 gives results of experiments using the modified hot plate, thin glass disks and the water cooled plate.

Table 1. Results Obtained with Thermal Precipitator,
Model I, and Magnesium Oxide Aerosols

Item No.	Spacing (in.)	Temperature		Sample Flow (cc./min.)	Deposit Length (in.)
		Hot Plate (°C)	Cold Plate (°C)		
1	0.005	71	28	150	0.28
2	0.005	80	30	300	0.44
3	0.005	75	30	450	0.59
4	0.010	82	20	79	0.50
5	0.010	72	20	112	0.22
6	0.010	76	34	142	0.20
7	0.010	76	25	150	0.28
8	0.010	50	7	151	0.44
9	0.010	67	20	154	0.80
10	0.010	44	-3	288	0.53
11	0.010	83	28	300	0.59
12	0.010	79	32	390	0.63
13	0.010	79	33	430	0.63
14	0.010	85	28	450	0.66
15	0.010	81	32	560	0.88
16	0.010	103	31	565	0.63
17	0.015	135	47	130	0.19
18	0.015	98	27	130	0.19
19	0.015	77	27	150	0.38
20	0.015	80	23	155	0.25
21	0.015	82	29	280	0.56
22	0.015	100	29	280	0.44
23	0.015	86	28	300	0.63
24	0.015	85	28	300	0.63
25	0.015	87	29	450	0.88
26	0.020	83	23	150	0.28
27	0.020	89	25	300	0.60
28	0.020	93	26	450	0.94

Thermal Precipitator, Model II.---The necessity of placing the Model I precipitator in the atmosphere to be sampled proved to be awkward and inconvenient; therefore, a second device was built. This device, shown in Figures 2 and 3 consisted of three primary parts: the base or cold plate, an insulating spacer and the upper plate assembly or hot plate. The base was a hollow disk through which cooling water was circulated. A circular cavity, three inches in diameter and 0.008 inch in depth was machined in the upper surface of the base for positioning a glass disk of these same dimensions. The top of the plate had four regularly spaced studs around its periphery for attaching the rest of the sampler. The insulating spacer separated the two surfaces and served to form a manifold-like space with the upper plate assembly, so that the aerosol flowed evenly outward in all directions from the inlet. A tube in the side of the spacer served as the exhaust port. The hot-plate or upper plate assembly consisted of a commercial disk heating element soldered to a machined brass plate. When in place, the underside of the outer edge of this piece made an airtight seal with the insulating spacer. A central tube acted as the inlet to the sampler. The temperature of the hot surface was controlled with a variable transformer. The spacing between the hot and cold surfaces was varied by using brass shims of different thicknesses between the insulating spacer and the upper-plate assembly.

The first model of this sampler (Model II) had a taper machined into the hot plate similar to the one in Model I. However, in this case, the flat portion was a ring one-quarter of an inch wide on the

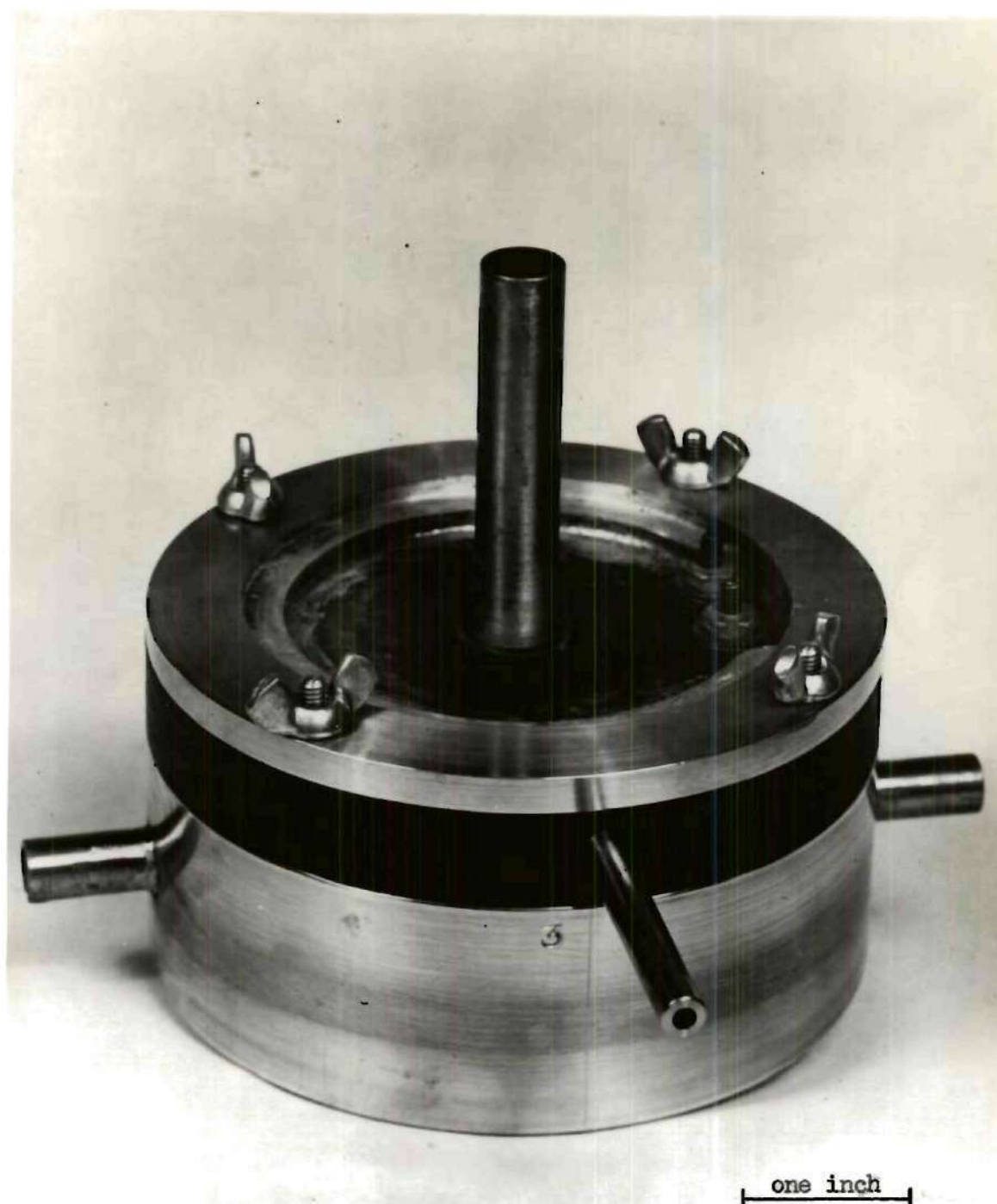


Figure 2. Thermal Precipitator, Model II.

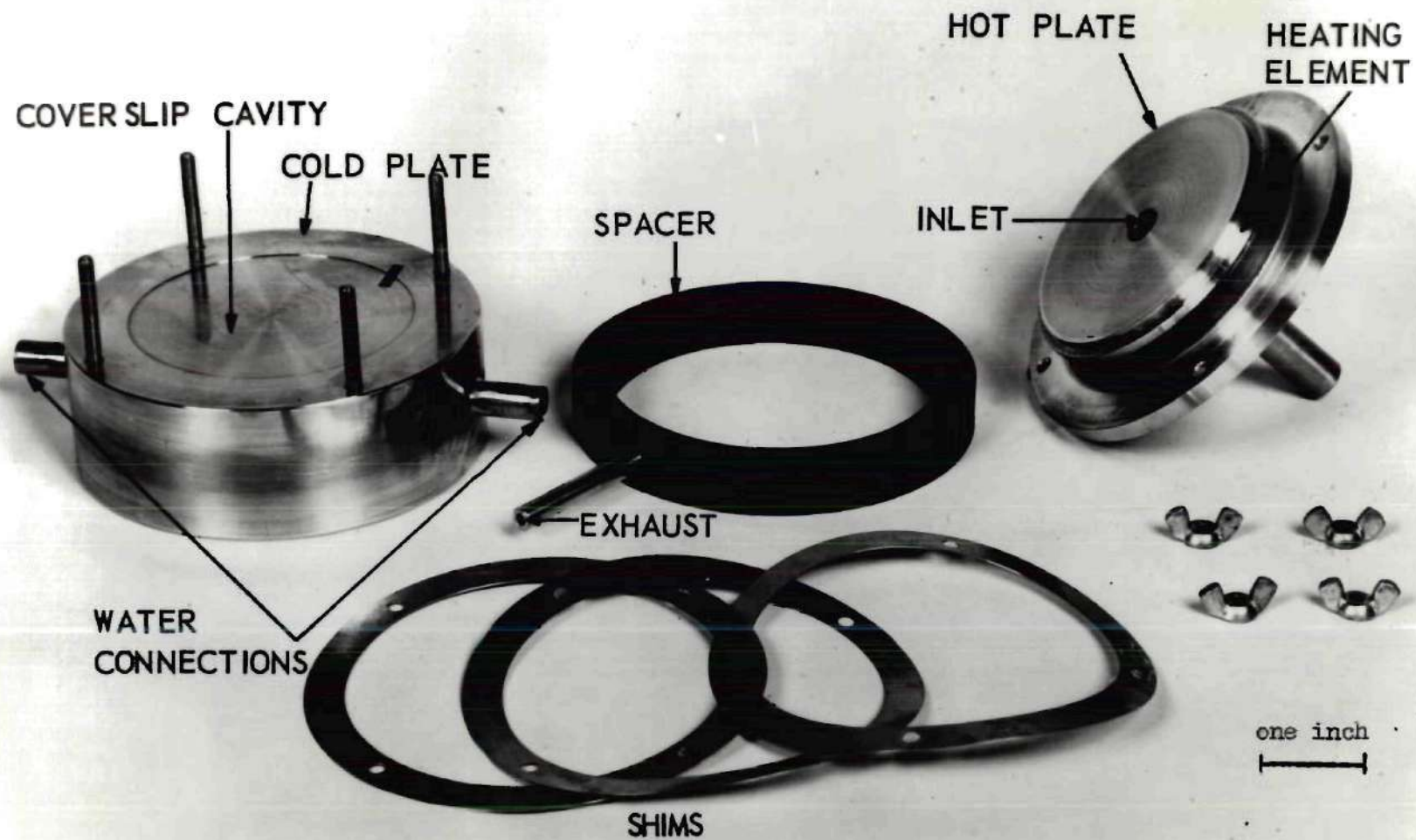


Figure 3. The Components of Thermal Precipitator, Model II.

outer part of the plate. Thus the edge of inlet opening in the center of the plate was 0.020 inch above the flat portion. This device was tested using magnesium oxide aerosols which were generated and aged as described above. Results of these tests are given in Table 2.

In subsequent models of this precipitator, the hot plate was not tapered. This model was designated as the Thermal Precipitator, Model IIa. With the Model IIa precipitator, a variety of aerosols were sampled. Liquid aerosols were generated with a DeVilbiss No. 180 nebulizer. Magnesium oxide aerosols were generated as described previously. With all aerosols used, a sample of about a liter gave sufficiently dense deposits. Table 3 gives the pertinent physical properties of the aerosol materials used.

With both the Model II and Model IIa precipitators, thermocouples installed in the hot and cold plates indicated the temperatures of the respective surfaces. Tables 4, 5, 6 and 7 present results obtained with the Model IIa precipitator.

Table 2. Results Obtained with Thermal Precipitator,
Model II, and Magnesium Oxide Aerosols

Item No.	Spacing (in.)	Temperature		Sample Flow (cc./min.)	Deposit Length (in.)
		Hot Plate (°C)	Cold Plate (°C)		
1	0.010	85	32	150	0.56
2	0.010	83	33	300	0.88
3	0.010	88	32	300	0.79
4	0.010	87	33	450	0.98
5	0.015	96	27	150	0.56
6	0.015	82	30	300	0.91
7	0.015	84	31	450	1.09
8	0.018	58	22	311	1.13
9	0.018	84	22	311	1.00
10	0.018	109	24	311	0.91
11	0.018	120	20	500	0.56
12	0.020	85	29	150	0.75
13	0.020	83	29	300	0.97
14	0.020	83	30	450	1.20
15	0.023	114	24	142	0.63
16	0.023	130	24	142	0.50
17	0.023	118	24	311	0.91

Table 3. Physical Properties of Aerosol Materials

Item No.	Material	Density ^a (gm/cm ³)	Thermal Conductivity ^b (gm-cal/cm-sec-°C)
1	Magnesium Oxide ^c	0.8	1.46 x 10 ⁻³
2	Diethylene Glycol	1.1	0.63 x 10 ⁻³
3	Mineral Oil	0.9	0.33 x 10 ⁻³
4	<u>Serratia marcescens</u> ^d	1.0	1.48 x 10 ⁻³
5	"Celite" ^e	1.5	0.82 x 10 ⁻³
6	Air	---	0.066 x 10 ⁻³

^aSee reference (19) in the bibliography.

^bSee reference (15) in the bibliography.

^cThe properties of powdered magnesia were used.

^dThe properties of bacteria were assumed to be that of water.

^eThe properties of this material were assumed to be those of quartz sand.

Table 4. Results Obtained with Thermal Precipitator,
Model IIA, and Magnesium Oxide Aerosols

Item No.	Spacing (in.)	Temperature		Sample Flow (cc./min.)	Deposit Length (in.)
		Hot Plate (°C)	Cold Plate (°C)		
1	0.005	68	15	120	0.39
2	0.005	90	32	150	0.37
3	0.005	80	30	150	0.16
4	0.005	98	26	150	0.13
5	0.005	80	30	300	0.62
6	0.005	83	28	300	0.23
7	0.005	102	31	300	0.20
8	0.005	81	31	450	0.80
9	0.005	82	32	450	0.31
10	0.005	101	31	450	0.25
11	0.008	65	20	300	0.63
12	0.010	83	33	150	0.34
13	0.010	80	30	150	0.21
14	0.010	100	31	150	0.15
15	0.010	80	31	150	0.18
16	0.010	80	31	150	0.20
17	0.010	37	20	200	0.79
18	0.010	40	20	250	0.87
19	0.010	82	32	300	0.66
20	0.010	80	31	300	0.40
21	0.010	80	31	300	0.39
22	0.010	100	31	300	0.29
23	0.010	39	20	300	1.14
24	0.010	46	20	300	0.59
25	0.010	40	20	300	0.98
26	0.010	42	20	300	1.18
27	0.010	84	32	450	0.84
28	0.010	80	31	450	0.48
29	0.010	80	31	450	0.47
30	0.010	100	31	450	0.40
31	0.010	64	21	500	1.18
32	0.010	75	21	500	0.71
33	0.010	114	15	600	0.59
34	0.010	111	15	700	0.71
35	0.010	117	15	860	0.79
36	0.010	140	15	1000	0.63

(continued)

Table 4. Results Obtained with Thermal Precipitator,
Model IIA, and Magnesium Oxide Aerosols
(concluded)

Item No.	Spacing (in.)	Temperature		Sample Flow (cc./min.)	Deposit Length (in.)
		Hot Plate (°C)	Cold Plate (°C)		
37	0.013	95	31	400	0.71
38	0.015	80	30	150	0.23
39	0.015	100	30	150	0.19
40	0.015	80	30	300	0.48
41	0.015	100	30	300	0.32
42	0.015	80	30	450	0.61
43	0.015	100	31	450	0.45
44	0.018	92	30	400	0.87
45	0.020	100	30	150	0.19
46	0.020	80	30	150	0.26
47	0.020	100	30	300	0.40
48	0.020	80	30	300	0.49
49	0.020	100	30	450	0.48
50	0.020	80	30	450	0.66

Table 5. Results Obtained with Thermal Precipitator,
Model IIA, and Diethylene Glycol Aerosols

Item No.	Spacing (in.)	Temperature		Sample Flow (cc./min.)	Deposit Length (in.)
		Hot Plate (°C)	Cold Plate (°C)		
1	0.005	62	15	270	0.31
2	0.005	92	15	300	0.39
3	0.005	62	15	500	0.59
4	0.005	112	15	660	0.59
5	0.005	72	15	900	0.59
6	0.005	70	15	1300	0.94
7	0.013	68	27	400	0.19
8	0.013	67	28	800	0.89

Table 6. Results Obtained with Thermal Precipitator,
Model IIA, and Mineral Oil Aerosols

Item No.	Spacing (in.)	Temperature		Sample Flow (cc./min.)	Deposit Length (in.)
		Hot Plate (°C)	Cold Plate (°C)		
1	0.005	104	37	100	0.24
2	0.010	54	30	150	0.53
3	0.010	87	38	300	0.53
4	0.010	145	41	400	0.67
5	0.010	86	38	600	0.80
6	0.010	65	27	700	0.91
7	0.020	100	36	300	0.87
8	0.020	96	36	300	0.79
9	0.020	117	36	300	0.59

Table 7. Results Obtained with Thermal Precipitator,
Model IIA, and Serratia marcescens
Bacterial Aerosols

Item No.	Spacing (in.)	Temperature		Sample Flow (cc./min.)	Deposit Length (in.)
		Hot Plate (°C)	Cold Plate (°C)		
1	0.010	74	32	400	0.59
2	0.010	84	22	325	0.94
3	0.015	134	45	200	0.59
4	0.015	108	37	200	0.20
5	0.015	118	36	200	0.28
6	0.015	99	35	500	0.79

CHAPTER III

DISCUSSION OF RESULTS

Previous Mathematical Analyses of Thermal Precipitation.--Cawood (6)

derived an equation for the time it would take a particle in a gas to move from a heated surface to the edge of the "dark space." A resumé of Cawood's derivation follows:

A spherical smoke or dust particle in the middle of a space in a temperature gradient will be bombarded by gas molecules moving in all directions, but consider only the bombardments due to molecules moving parallel to the gradient, and if F is the force per unit area (i.e., area normal to the gradient), then the total force on the one side of the spherical particle is

$$\int_0^{\pi/2} F 2\pi r^2 \sin \theta \cos \theta d\theta = F\pi r^2 . \quad (1)$$

The force on the particle due to the bombardment of the gas molecules may now be calculated in a similar manner to that in which Einstein (10) calculated the force on a vane radiometer. Thus $\frac{1}{6} N_1 C_1 (\pi r^2)$ molecules will collide with the particle on one side and $\frac{1}{6} N_2 C_2 (\pi r^2)$ on the other, where N and C refer to the number of molecules and their average velocity respectively. The difference of velocities of the molecules accounts for the heat flow.

The heat flow, if the particle was not there, may be written

$$\pi r^2 f = \frac{1}{6} N_1 C_1 (\pi r^2) \frac{m C_1^2}{2} - \frac{1}{6} N_2 C_2 (\pi r^2) \frac{m C_2^2}{2} . \quad (2)$$

If C_1 and C_2 are the velocities appropriate to the temperatures at the place of the last collision,

$$\frac{1}{2} m C^2 = \frac{3}{2} R T \quad (3)$$

and

$$\frac{1}{2} m (C_1^2 - C_2^2) = - \frac{3}{2} R \frac{dT}{dx} 2\lambda , \quad (4)$$

$$f = - \frac{1}{2} N_1 C_1 R \frac{dT}{dx} \lambda . \quad (5)$$

If now we consider the particle, there will be an excess of momentum away from the hot plate which is equal to

$$\frac{1}{6} N_1 C_1 (\pi r^2) [m C_1 - m C_2] , \quad (6)$$

and if the impulse due to recoil is neglected, then the force on the particle will be

$$\frac{\pi r^2 f}{C} \quad (7)$$

or

$$- \frac{1}{2} N_1 R \frac{dT}{dx} 2\pi r^2 \left(\text{if } C = \frac{C_1 + C_2}{2} \text{ and } C \text{ is very nearly } = C_1 \right) \quad (8)$$

or

$$-\frac{1}{2} P \frac{dT}{dx} \frac{\lambda}{T} r^2 . \quad (9)$$

If a smoke particle moves under a constant force F , however, it may be written that

$$F = \frac{6\pi\mu r v}{1 + \frac{A\lambda}{r}} . \quad (10)$$

Also, as the edge of the dark space acts as a semi-permeable membrane, then the smoke as a whole exerts an osmotic pressure on the edge of the space equal to $\frac{RT}{N} n$. For one particle, this is the component of the Brownian motion on the edge and is, therefore, $\frac{RT}{N}$ and the force of one particle on the space is $\frac{RT}{N} \pi r^2$. Consequently,

$$\frac{1}{2} P \frac{dT}{dx} \frac{\lambda}{T} \pi r^2 = \frac{6\pi\mu r v}{1 + \frac{A\lambda}{r}} + \frac{RT}{N} \pi r^2 \quad (11)$$

or

$$v = \frac{\frac{1}{2} P \frac{dT}{dx} \frac{\lambda}{T} \pi r^2 - \frac{RT}{N} \pi r^2}{6\pi\mu r} \left(1 + \frac{A\lambda}{r} \right) . \quad (12)$$

This equation neglects the presence of convection currents and also, although the velocity appears to be proportional to the radius of the particle, this is not actually the case. This derivation parallels Einstein's (10) calculation of the force on a vane radiometer and, therefore, has the same limitations, that is, a fundamental assumption

is that the radius of the particle should be of the same order of magnitude as the mean free path of the gas or approximately 1×10^{-5} centimeters.

If the temperature gradient is linear over the region of the dark space, then the time taken for a particle to move from the hot surface to the edge of the dark space may be calculated as follows. From the last equation, i.e. (12), neglecting the $\frac{RT}{N} \pi r^2$ term,

$$v' = \frac{dx}{dt} = \frac{v}{T} , \quad (13)$$

and if $\frac{dT}{dx}$ is constant, then

$$T_x = \frac{dT}{dx} x + T_a , \quad (14)$$

$$\frac{dx}{dt} = \frac{v}{\frac{dT}{dx} x + T_a} , \quad (15)$$

$$t = \frac{dT}{dx} \frac{x^2}{2} + T_a x \frac{1}{v} , \quad (16)$$

or substituting the expression v in Equation (12),

$$t = \frac{\frac{dT}{dx} \frac{x^2}{2} + T_a x}{P \frac{dt}{dx} r \left(1 + \frac{A\lambda}{r} \right)} 12\mu . \quad (17)$$

Cawood stated:

While the above gives the explanation of why the particles move away from a hot body, it does not enable one to calculate the width of the dark space. This appears to be almost impossible because it obviously depends so much upon convection current, and consequently the design of the apparatus.

Watson (25) suggested an empirical relationship of the form

$$x = B \Delta T Q^{\alpha} \quad (18)$$

to define the thickness of the dark space. The Constants B and α were evaluated for various shape hot bodies. The empirical equations arrived at for the different objects were

$$x = 7.6 \times 10^{-5} \Delta T Q^{-0.38} \quad (19)$$

for horizontal rods and

$$x = 15.6 \times 10^{-5} \Delta T Q^{-0.38} \quad (20)$$

for vertical plane surfaces. The units in the preceding two equations are in the c.g.s. system. This investigator (25) also presented the results of experiments which led to the conclusion that the width of the dark space varied as the -0.65 power of the absolute pressure. As a result of these studies, Watson concluded that the width of the dust-free space was independent of the nature of the dust or of the particle size and that it is a function of the size and shape of the hot body.

Harrington and Crozier (14) utilized Cawood's equation for the time required for a particle to move from a hot plate to a distance x to obtain an equation with which to correlate the results obtained with an areal type precipitator. Equation (17) was modified by replacing the Cunningham correction term to Stokes' Law by a factor C_m which depends on particle size. This factor is unity for particle sizes greater than three microns diameter. The equation now becomes

$$t = \frac{12\mu}{P\lambda D_p C_m} \left(x^2 + \frac{2Tx}{\frac{dT}{dx}} \right). \quad (21)$$

The derivation of Harrington and Crozier follows. Consider a thermal precipitator comprising two flat plates of width w separated by a distance x , with a thermal gradient giving an average velocity v to a particle between the plates. Air passes between the plates in the direction perpendicular to w , with velocity u . The air flow is given by wxu and the area in which all the particles are collected is $\frac{wxu}{v}$. Then a figure of merit, defined as the volume of air processed per unit time per unit area of deposit, is

$$E = \frac{\text{Flow rate}}{\text{Area of collection}} = \frac{wxu}{\frac{wxu}{v}} = v, \quad (22)$$

or based on Cawood's equation,

$$E = v = \frac{x}{t} = \frac{P\lambda C_m}{12\mu} \left(x + \frac{1}{\frac{2T}{dT/dx}} \right). \quad (23)$$

An approximation for small values of x is that

$$T = \frac{T_h + T_c}{2}, \quad (24)$$

and

$$\frac{dT}{dx} = \frac{T_h - T_c}{x}. \quad (25)$$

Then

$$E = \frac{P\lambda C_m}{2l\mu} \left(1 - \frac{T_c}{T_h} \right) \frac{D_p}{x} . \quad (26)$$

In this investigation, good agreement between experimental results and calculated results was not obtained with the above equation. However, when the cold plate was water cooled instead of air cooled, the agreement was much improved.

The paper of Saxton and Ranz (23) summarized Epstein's (11) derivation of the radiometer force for a sphere which was large relative to the mean free path of the medium. Epstein, recognizing the kinetic and hydrodynamic aspects of thermal repulsion, took into account the fact that the behaviour of a body suspended in a gas and in a thermal field depends on the ratio of heat transported through the particle's interior (internal conduction) to the heat received in unit time from molecular impacts. Therefore, the thermal conductivities of the gas and the immersed material should enter into the derivation of the thermal force. In addition to the assumption that the particle was large relative to the mean free path of the gas, other assumptions were that a uniform temperature gradient existed in the gas at a great distance from the particle and that Fourier's equation for heat conduction without convection could be used even though such a state could not exist because of the thermal creep. Epstein then broke down the problem into two phases of hydrodynamics and heat conduction which were treated independently at first, but later combined through the concept of thermal

creep.

The concept of thermal creep was due to Maxwell (18) who deduced that, since at any gas-solid interface, molecules are continuously adsorbing on and desorbing from the solid surface, a temperature gradient existing along the surface would cause the desorbing molecules to have a greater component of velocity in the direction of the increasing surface temperature than when they arrived at the surface. Thus, as a consequence of the interaction of the gas layers close to the surface with the unequally heated solid, there would be a creeping flow of gas over the surface from the colder to the warmer regions. Because this movement arises from a gas-surface interaction, the surface must itself experience a tangential force directed toward the colder regions.

Epstein solved the heat conduction problem to obtain the temperature gradient over the surface of the sphere in terms of that prevailing in the gas. From this could then be calculated the velocity of thermal creep. Next the Navier-Stokes equations of motion were solved with the assumption that the inertia terms are negligible and with the creep velocity at the surface of the sphere as a boundary condition. The thermal force was then found as the integral over the surface of the component of force parallel to the direction of heat flow. The expression for thermal force then, as derived by Epstein is

$$F_T = 9\pi \frac{D_p}{2} \frac{\mu^2}{\rho T} \frac{k}{2k + k_p} \frac{\Delta T}{x} \quad (27)$$

Experiments of Saxton and Ranz confirming this equation are described in the Introduction.

Mathematical Analysis of Areal-Type Thermal Precipitators.—The statement given above in terms of the physical properties of the gas and the particle allows the development of equations of motion for particles suspended in a gas and subjected to thermal and other forces. Consider a spherical particle moving at its terminal velocity in a fluid in which a thermal gradient exists and in which gravitational forces are non-existent. Since the particle is at its terminal velocity, the forces exerted on the particle are in equilibrium. These are the forces due to temperature gradient and viscous drag. Thus

$$F_V = F_T , \quad (28)$$

but

$$F_V = \frac{3\pi\mu D_p v}{C_m} , \quad (29)$$

and

$$F_T = 9\pi \frac{D_p}{2} \frac{\mu^2}{\rho T} \frac{k}{2k + k_p} \frac{\Delta T}{x} . \quad (27)$$

Substituting Equations (27) and (29) in Equation (28) gives

$$\frac{3\pi\mu D_p v}{C_m} = \frac{9}{2} \pi D_p \frac{\mu^2}{\rho T} \frac{k}{2k + k_p} \frac{\Delta T}{x} , \quad (30)$$

or rearranging

$$v = \frac{3}{2} C_m \frac{\mu}{\rho T} \frac{k}{2k + k_p} \frac{\Delta T}{x} , \quad (31)$$

but at moderate temperatures and atmospheric pressure

$$\rho \approx \frac{MP}{RT} , \quad (32)$$

and Equation (31) becomes

$$v = \frac{3}{2} C_m \frac{R\mu}{MP} \frac{k}{2k + k_p} \frac{\Delta T}{x} . \quad (33)$$

This last equation confirms conclusions of other investigators that the motion of a particle in a thermal field only, is independent of particle size except below three microns, directly proportional to thermal gradient, and inversely proportional to total gas pressure. It also shows that this motion is not independent of the material, since, in Equation (33), the particle velocity is inversely proportional to the thermal conductivity of the particle.

Consider, now, a particle in both a thermal and a gravitational field acting in the same direction, i.e., "down." The equation of equilibrium is now

$$F_V = F_G + F_T . \quad (34)$$

But

$$F_G = \frac{D_p^3 (\rho_p - \rho) g}{6} , \quad (35)$$

and F_V and F_T are defined above. Substituting Equations (27), (29), and (35) in Equation (34) gives

$$\frac{3\pi\mu D_p v}{C_m} = \frac{\pi D_p^3 (\rho_p - \rho) g}{6} + \frac{9}{2} \pi D_p \frac{\mu^2}{\rho T} \frac{k}{k + k_p} \frac{\Delta T}{x}, \quad (36)$$

or, rearranging

$$v = \frac{D_p^2 C_m (\rho_p - \rho) g}{18\mu} + \frac{3}{2} C_m \frac{\mu}{\rho T} \frac{k}{k + k_p} \frac{\Delta T}{x}. \quad (37)$$

In the term $(\rho_p - \rho)$, ρ is very small compared to ρ_p and can be neglected. Also, the approximation of ρ , mentioned previously, can be used where it appears alone. Therefore,

$$v = \frac{D_p^2 C_m \rho_p g}{18\mu} + \frac{3}{2} C_m \frac{R\mu}{MP} \frac{k}{2k + k_p} \frac{\Delta T}{x}. \quad (38)$$

This, then, is the equation for the terminal velocity of a particle in a thermal precipitator of the areal type which has the hot and cold plates perpendicular to the gravitational field and the hot plate "above" the cold plate.

In order to obtain v in terms of the shape of the thermally precipitated deposit and the geometry of the sampler, a particle in a particular sample as is illustrated in Figure 4 must be considered. The first calculation will be for the Model IIa sampler. The instantaneous horizontal velocity of the particle is

$$u = \frac{U}{2\pi x_0 (z + r_0)}, \quad (39)$$

or

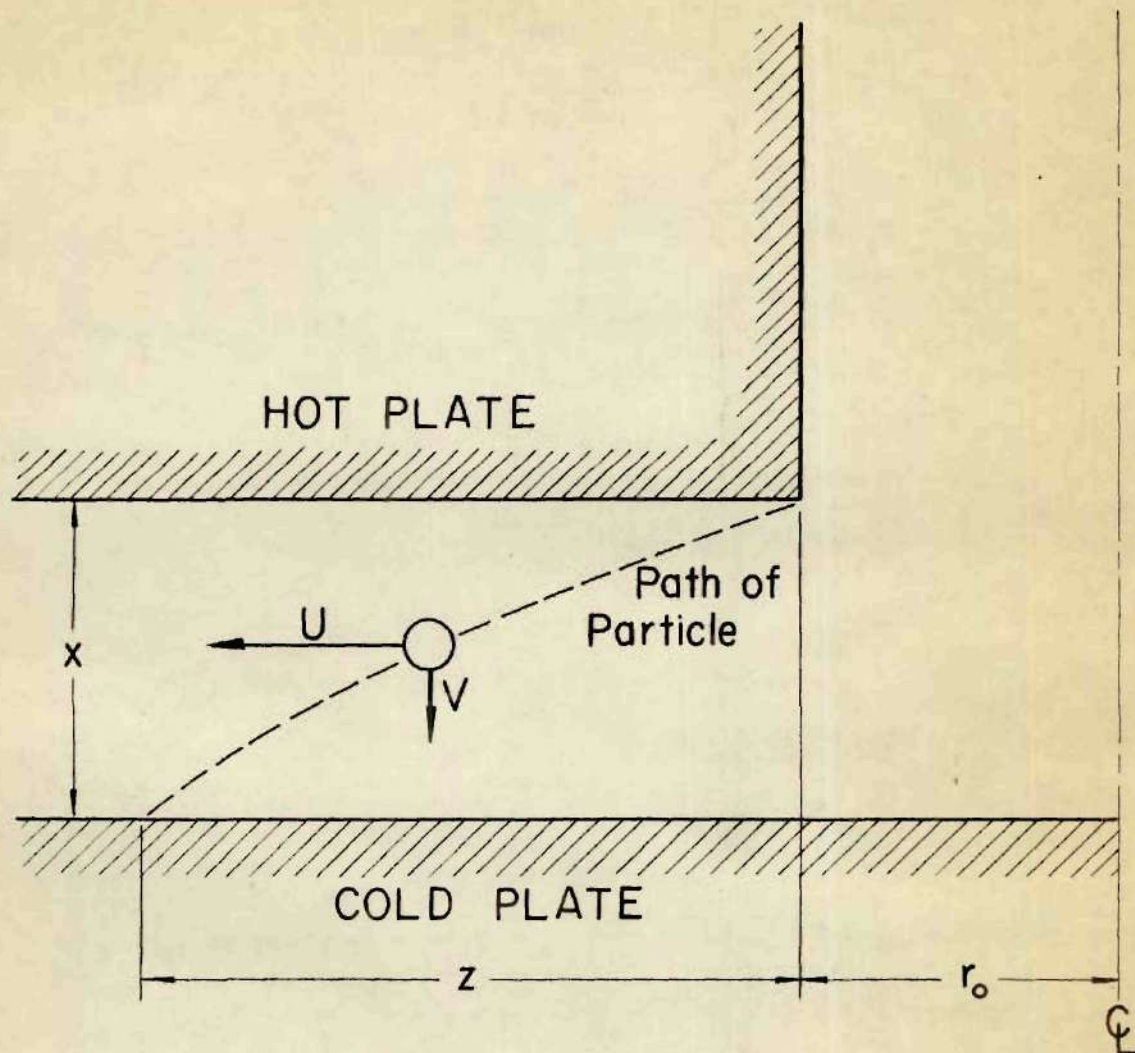


Figure 4. Diagrammatic Sketch of Thermal Precipitator, Model IIa.

$$\frac{dz}{dt} = \frac{U}{2\pi x_0 (z + r_0)} \quad (40)$$

Separating variables and integrating between limits,

$$\int_0^z (z + r_0) dz = \frac{U}{2\pi x_0} \int_0^t dt \quad (41)$$

$$z (z + 2r_0) = \frac{Ut}{\pi x_0} \quad (42)$$

or

$$t = \frac{\pi x_0 z (z + 2r_0)}{U} \quad (43)$$

In this same time the particle traverses the distance x_0 , or

$$t = \frac{x_0}{v} \quad (44)$$

Since Equations (43) and (44) are equal,

$$\frac{x_0}{v} = \frac{\pi x_0 z (z + 2r_0)}{U} \quad (45)$$

and rearrangement shows that

$$v = \frac{U}{\pi z (z + 2r_0)} \quad (46)$$

For Model I,

$$v = \frac{U (x_0 + \partial)}{2\pi z \left[r_0 (x_0 + \partial) - \left(x_0 + \partial - \frac{r_0 \partial}{z_0} \right) \frac{z}{2} + \frac{\partial}{z_0} \frac{z^2}{3} \right]} \quad (47)$$

For Model II,

$$v = \frac{U (x_0 + \partial)}{2\pi z \left[r_0 (x_0 + \partial) + \left(x_0 + \partial - \frac{r_0 \partial}{z_0} \right) \frac{z}{2} - \frac{\partial}{z_0} \frac{z^2}{3} \right]} \quad (48)$$

Equations (46), (47) and (48) assume that all particles at the periphery of the deposit started from a point at the inner edge of the hot surface as indicated in Figure 4. Complete derivations of Equations (47) and (48) appear in the Appendix.

Tables 8, 9, 10, 11, 12 and 13 present the results of treating the experimental data with Equations (46), (47) and (48). Figures 5, 6, 7, 8, 9 and 10 are plots of the experimental terminal velocity, v , using Equations (46), (47) and (48), versus the experimental temperature gradient. The indicated lines were obtained by substituting suitable values in Equation (38). For the precipitators which had a sloping segment in the hot plate, an average spacing, x , was used to obtain the temperature gradient.

Due to the poly-dispersity of particle sizes, data obtained when working with aerosols are difficult to correlate with operating variables. The current investigation is an example of this fact. It is possible for each item in the tables of results to correspond to a different diameter particle. In addition, each terminal velocity obtained, using the proper equation which corresponds to the thermal

Table 8. Calculated Results with Thermal Precipitator,
Model I, and Magnesium Oxide Aerosols

Item No.	ΔT (°C)	$x_{ave.}$ (in.)	$\frac{\Delta T}{x_{ave.}}$ (°C/cm.)	$\frac{v}{\bar{U}}$ (1/cm. ²)	v^a (cm./sec.)
1	43	0.022	770	0.073	0.18
2	50	0.020	980	0.054	0.27
3	45	0.018	980	0.046	0.35
4	62	0.024	1020	0.048	0.06
5	52	0.028	730	0.087	0.16
6	42	0.028	590	0.094	0.22
7	51	0.027	740	0.073	0.18
8	43	0.025	680	0.052	0.13
9	47	0.021	880	0.038	0.10
10	47	0.024	770	0.047	0.22
11	55	0.023	940	0.044	0.22
12	47	0.023	800	0.043	0.28
13	46	0.023	790	0.043	0.31
14	57	0.022	1020	0.042	0.31
15	49	0.020	960	0.037	0.34
16	72	0.023	1230	0.043	0.40
17	88	0.033	1050	0.097	0.21
18	71	0.033	850	0.097	0.21
19	50	0.031	640	0.056	0.14
20	57	0.032	700	0.077	0.20
21	53	0.029	720	0.043	0.20
22	71	0.030	930	0.051	0.24
23	58	0.028	820	0.041	0.21
24	57	0.028	800	0.041	0.21
25	59	0.025	930	0.035	0.27
26	60	0.037	640	0.070	0.18
27	64	0.033	760	0.041	0.20
28	67	0.020	1320	0.033	0.25

^aFrom Equation (47).

Table 9. Calculated Results with Thermal Precipitator,
Model II, and Magnesium Oxide Aerosols

Item No.	ΔT (°C)	$x_{ave.}$ (in.)	$\frac{\Delta T}{x_{ave.}}$ (°C/cm.)	$\frac{v}{U}$ (1/cm. ²)	v^a (cm./sec.)
1	53	0.025	840	0.122	0.31
2	50	0.022	900	0.066	0.33
3	56	0.023	960	0.075	0.38
4	54	0.021	1010	0.057	0.43
5	69	0.030	900	0.108	0.27
6	52	0.026	790	0.059	0.30
7	53	0.025	830	0.047	0.35
8	36	0.027	530	0.044	0.23
9	62	0.029	840	0.050	0.26
10	85	0.029	970	0.057	0.30
11	100	0.033	1200	0.108	0.90
12	56	0.033	670	0.072	0.18
13	54	0.031	690	0.051	0.26
14	53	0.029	720	0.039	0.29
15	90	0.037	960	0.090	0.21
16	106	0.038	1100	0.126	0.30
17	94	0.034	1090	0.054	0.28

^aFrom Equation (48).

Table 10. Calculated Results with Thermal Precipitator,
Model IIA, and Magnesium Oxide Aerosols

Item No.	ΔT (°C)	x (in.)	$\frac{\Delta T}{x}$ (°C/cm.)	$\frac{v}{U}$ (1/cm. ²)	v^a (cm./sec.)
1	43	0.005	3390	0.16	0.32
2	62	0.005	4890	0.18	0.45
3	50	0.005	3940	0.56	1.40
4	72	0.005	5680	0.74	1.85
5	50	0.005	3940	0.08	0.40
6	55	0.005	4330	0.36	1.80
7	71	0.005	5600	0.43	2.15
8	50	0.005	3940	0.05	0.38
9	50	0.005	3940	0.23	1.70
10	70	0.005	5520	0.31	2.33
11	45	0.008	2210	0.08	0.40
12	50	0.010	1970	0.20	0.50
13	50	0.010	1970	0.39	0.98
14	69	0.010	2720	0.60	1.50
15	49	0.010	1930	0.48	1.20
16	49	0.010	1930	0.43	1.08
17	17	0.010	670	0.05	0.17
18	20	0.010	790	0.05	0.21
19	50	0.010	1970	0.07	0.35
20	49	0.010	1930	0.16	0.80
21	49	0.010	1930	0.16	0.80
22	69	0.010	2720	0.25	1.25
23	19	0.010	750	0.03	0.15
24	26	0.010	1030	0.09	0.45
25	20	0.010	790	0.04	0.20
26	22	0.010	870	0.03	0.15
27	52	0.010	2050	0.05	0.38
28	49	0.010	1930	0.12	0.90
29	49	0.010	1930	0.13	0.98
30	69	0.010	2720	0.16	1.20
31	43	0.010	1690	0.03	0.25
32	54	0.010	2130	0.06	0.50
33	99	0.010	3900	0.09	0.90
34	96	0.010	3780	0.06	0.70
35	102	0.010	4020	0.05	0.72
36	125	0.010	4920	0.08	1.33

(continued)

Table 10. Calculated Results with Thermal Precipitator,
Model IIA, and Magnesium Oxide Aerosols
(concluded)

Item No.	$\frac{\Delta T}{(\text{°C})}$	$\frac{x}{(\text{in.})}$	$\frac{\Delta T}{x}(\text{°C/cm.})$	$\frac{v}{U}(\text{l/cm.}^2)$	$\frac{v^a}{(\text{cm./sec.})}$
37	64	0.013	1940	0.06	0.40
38	50	0.015	1900	0.35	0.88
39	70	0.015	2670	0.45	1.13
40	50	0.015	1900	0.12	0.60
41	70	0.015	2670	0.18	0.90
42	50	0.015	1900	0.08	0.60
43	69	0.015	2630	0.13	0.97
44	62	0.018	1360	0.05	0.33
45	70	0.020	1380	0.45	1.13
46	50	0.020	980	0.30	0.75
47	70	0.020	1380	0.16	0.80
48	50	0.020	980	0.12	0.60
49	70	0.020	1380	0.12	0.90
50	50	0.020	980	0.07	0.52

^aFrom Equation (46).

Table 11. Calculated Results with Thermal Precipitator,
Model IIA, and Diethylene Glycol Aerosols

Item No.	$\frac{\Delta T}{(\text{°C})}$	$\frac{x}{(\text{in.})}$	$\frac{\Delta T}{x}(\text{°C/cm.})$	$\frac{v}{U}(\text{1/cm.}^2)$	$v^a(\text{cm./sec.})$
1	47	0.005	3700	0.23	1.04
2	77	0.005	6060	0.16	0.80
3	47	0.005	3700	0.09	0.75
4	127	0.005	10000	0.09	0.99
5	57	0.005	4490	0.09	1.35
6	55	0.005	4330	0.04	0.87
7	41	0.013	1240	0.45	3.00
8	39	0.013	1180	0.04	0.53

^aFrom Equation (46).

Table 12. Calculated Results with Thermal Precipitator,
Model IIA, and Mineral Oil Aerosols

Item No.	ΔT (°C)	x (in.)	$\frac{\Delta T}{x}$ (°C/cm.)	$\frac{v}{U}$ (1/cm. ²)	v^a (cm./sec.)
1	67	0.005	5280	0.34	0.57
2	24	0.010	950	0.10	0.25
3	49	0.010	1930	0.10	0.50
4	104	0.010	4090	0.07	0.47
5	48	0.010	1890	0.05	0.50
6	38	0.010	1500	0.04	0.47
7	64	0.020	1260	0.04	0.20
8	60	0.020	1180	0.05	0.25
9	81	0.020	1590	0.09	0.45

^aFrom Equation (46).

Table 13. Calculated Results with Thermal Precipitator,
Model IIA, and Serratia marcescens
Bacterial Aerosols

Item No.	$\frac{\Delta T}{(\text{°C})}$	$\frac{x}{(\text{in.})}$	$\frac{\Delta T}{x}(\text{°C/cm.})$	$\frac{v}{U}(\text{1/cm.}^2)$	$v^a(\text{cm./sec.})$
1	52	0.010	2050	0.09	0.60
2	62	0.010	2440	0.04	0.22
3	89	0.015	3390	0.09	0.30
4	71	0.015	2700	0.43	1.44
5	82	0.015	3120	0.27	0.90
6	64	0.015	2440	0.05	0.42

^aFrom Equation (46).

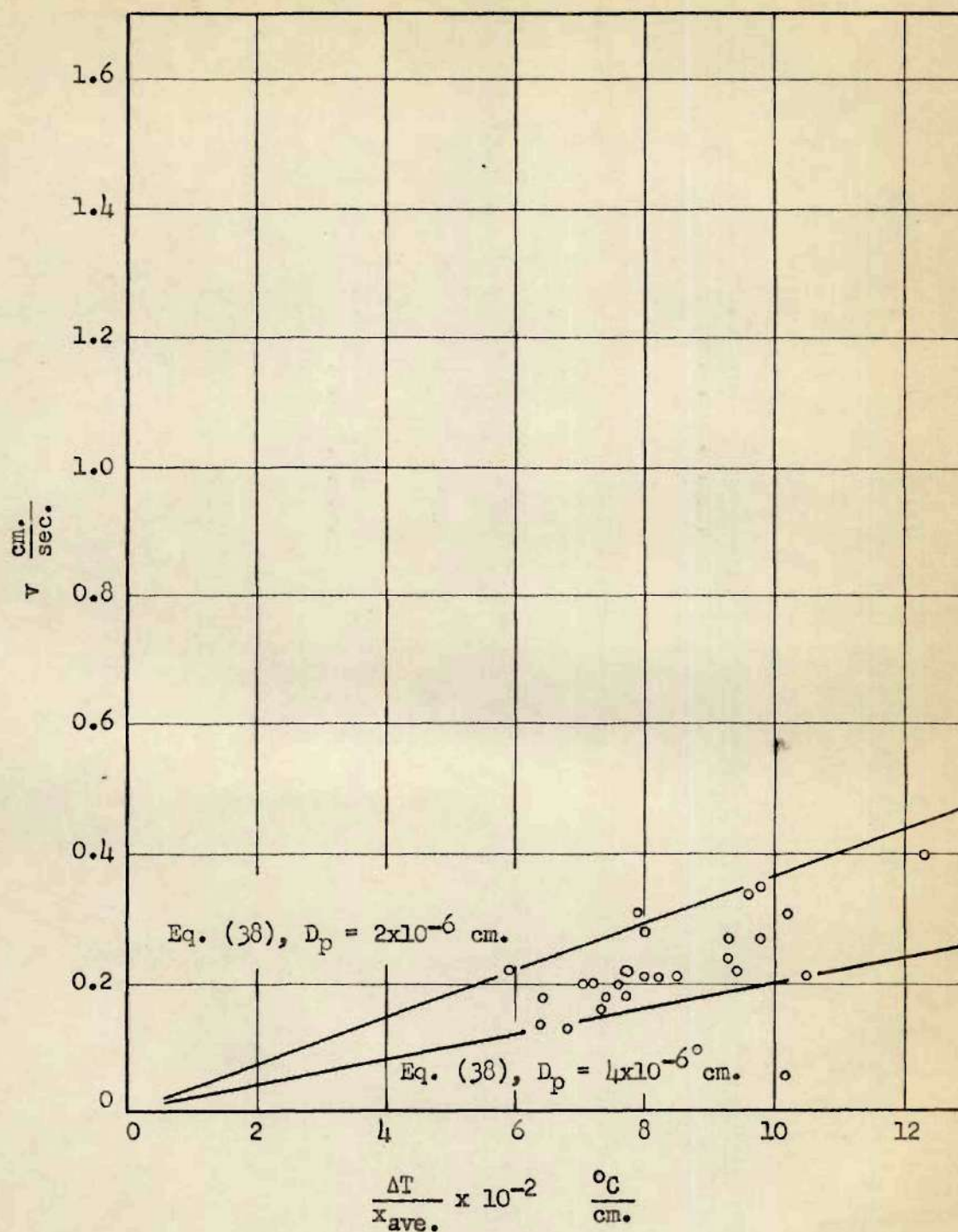


Figure 5. Results with Thermal Precipitator, Model I, and Magnesium Oxide Aerosols.

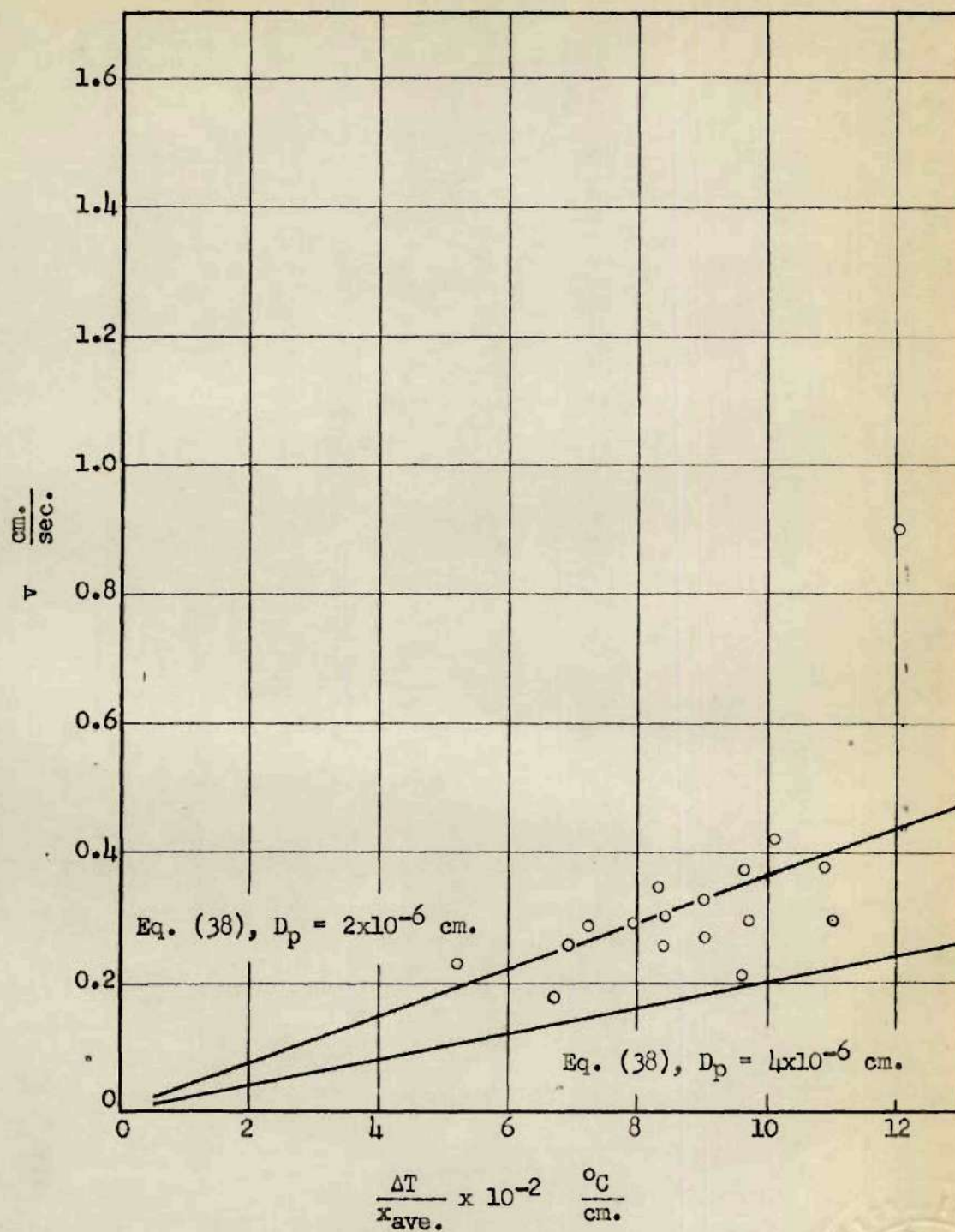


Figure 6. Results with Thermal Precipitator, Model II, and Magnesium Oxide Aerosols.

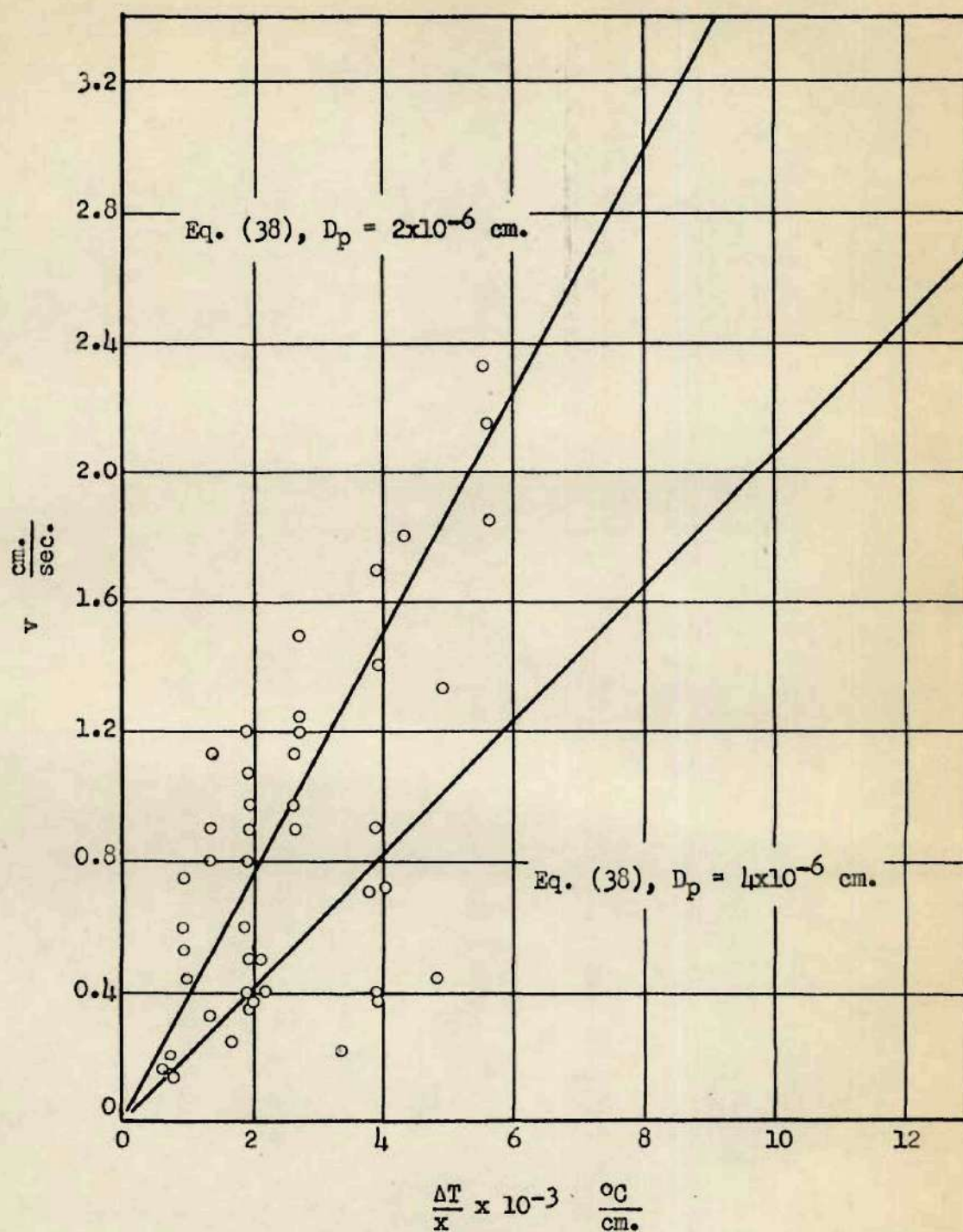


Figure 7. Results with Thermal Precipitator, Model IIa, and Magnesium Oxide Aerosols.

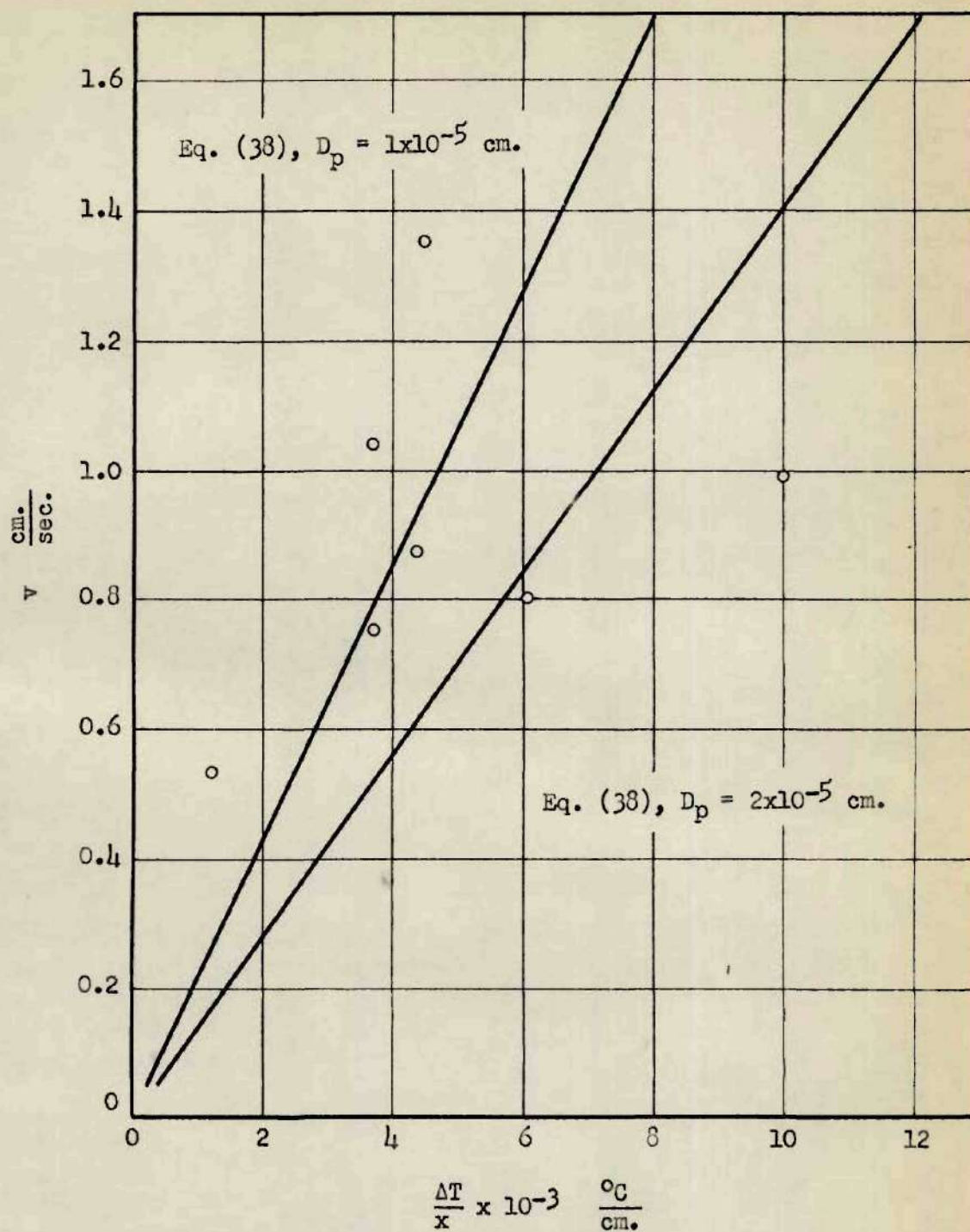


Figure 8. Results with Thermal Precipitator, Model IIa, and Diethylene Glycol Aerosols.

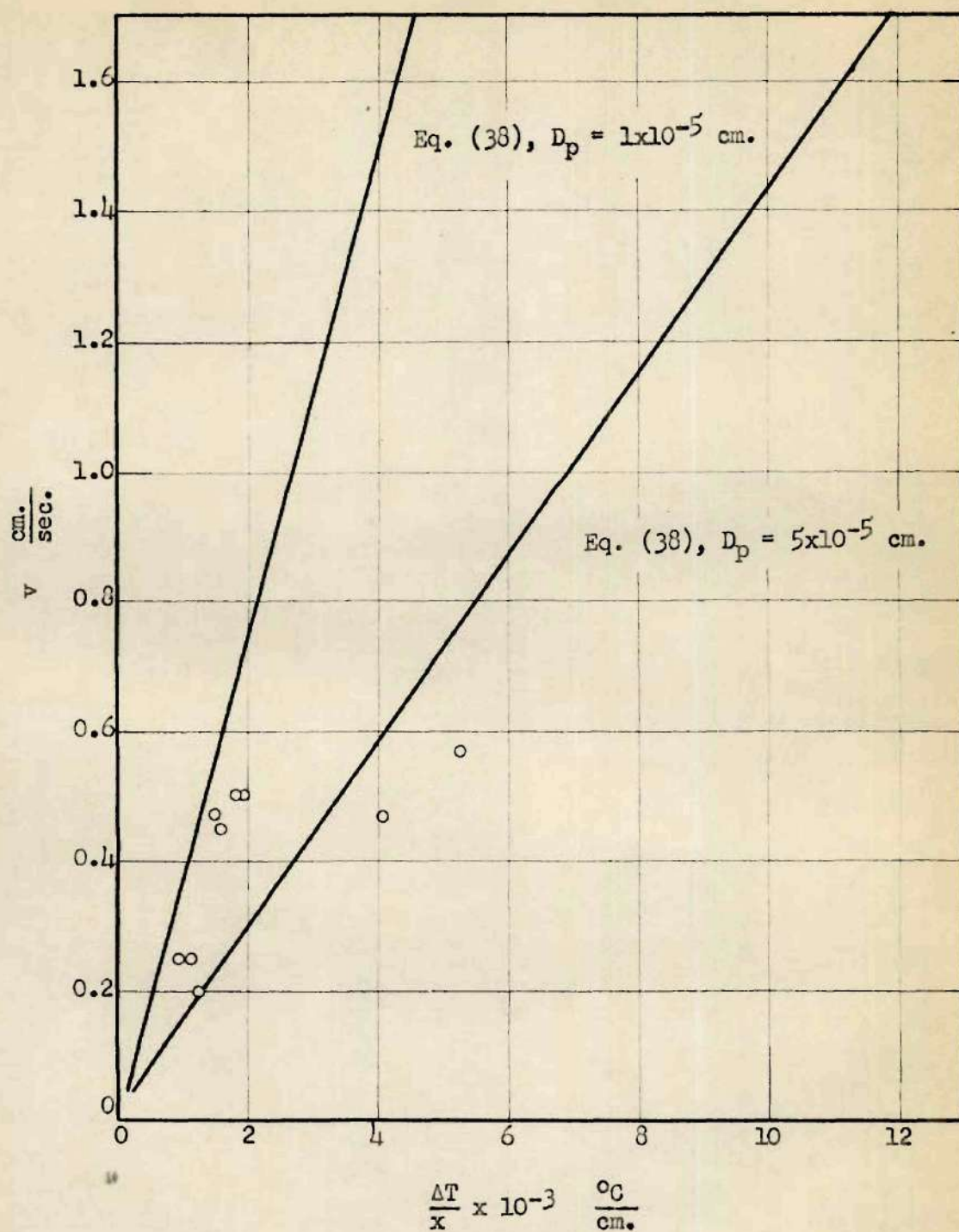


Figure 9. Results with Thermal Precipitator, Model IIa, and Mineral Oil Aerosols.

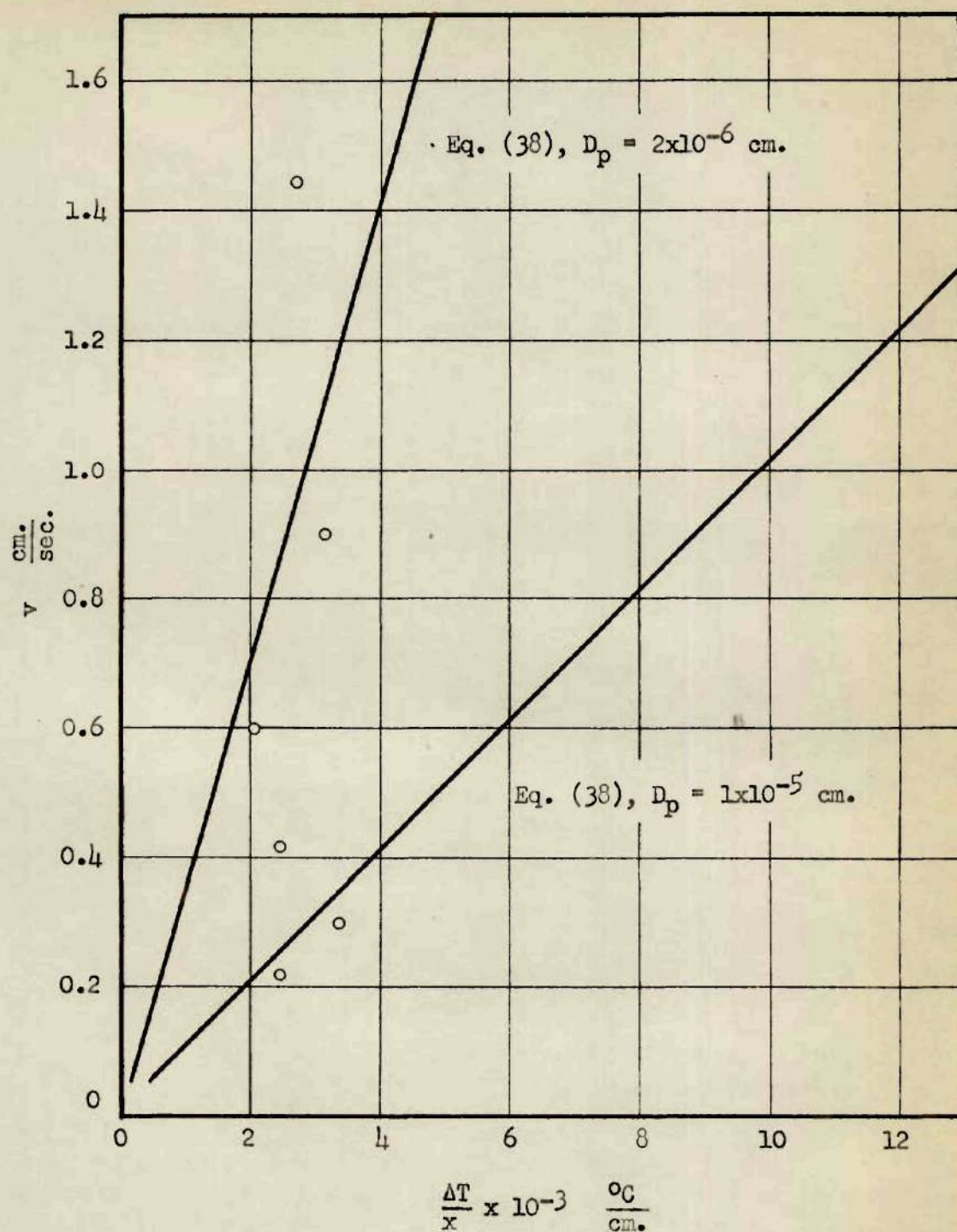


Figure 10. Results with Thermal Precipitator, Model IIa, and Serratia marcescens Bacterial Aerosols.

precipitator geometry, will lie on a line whose intercept, at a thermal gradient equal to zero, is a function of particle density, gas viscosity and particle diameter, i.e., of a particle deposited at the outer edge of the visible deposit. The slope of this line is a function of the gas viscosity, gas pressure, particle diameter (if particle diameter is less than 3×10^{-4} centimeters) and particle and gas thermal conductivity. Gas viscosity, particle density, and particle and gas thermal conductivity should be evaluated at the average temperature of the particle and the gas. That the data are grouped as closely as they are about a line calculated from Equation (38) that was evaluated at standard conditions and for one particle size, is evidence that experimental and theoretical results are in agreement. That is not to say that the particle diameter used in obtaining these lines, i.e., the ones presented in Figures 5, 6, 7, 8, 9 and 10, will be the true particle diameter at the outer edge of the deposits corresponding to the experimental points. This grouping of the data is due, in part, to the fact that the test aerosols were aged an appreciable time before they were used.

Microscopic examination of the deposits obtained from sampling bacterial aerosols showed that the outer edge of these deposits consisted, primarily, of sub-micron liquid droplets and no bacteria. This accounts for the small particle diameter indicated in Figure 10. In the deposits which were examined microscopically, including those obtained with magnesium oxide, these small liquid droplets were observed at the outer edge of the deposit, except in the runs where elevated

cold plate temperatures were used. These droplets were attributed to moisture condensation. There is a possibility that, even though the cold plate temperature is above the dew point of water vapor, there is a concentration of water vapor near the cold plate due to thermal diffusion which results in the above-mentioned condensation.

Attempts at checking the efficiency of Thermal Precipitator, Model IIa, by filtering the efflux of this precipitator with an asbestos filter, produced negative results. Aerosols of magnesium oxide were used. The filters were washed with diluted hydrochloric acid and analyzed for magnesium using the "versenate" method (3 and 9). This very sensitive test showed no magnesium oxide penetrating the thermal precipitator when this device was properly operated. The above are proof that all of the particulate matter is being removed from the sample stream.

Thus far, no technique has been developed for culturing bacteria from the surface of the glass cover slip. However, the bacteria can be readily observed with a phase-contrast optical microscope or an electron microscope. The Model IIa Thermal Precipitator is now being used for the routine examination of all types of aerosols, including bacterial, in the Micromeritics and Bioengineering Laboratories of the Engineering Experiment Station, Georgia Institute of Technology and at the Army Chemical Corps Laboratories, Camp Detrick, Frederick, Maryland.

Harrington and Crozier (14) present data obtained using an areal type thermal precipitator. For their precipitator, it can be shown that

$$v = \frac{U}{ZW} \quad . \quad (49)$$

However, in this case, thermal and gravitational forces were acting in opposition. Assuming the direction toward the cold surface to be positive,

$$v = - \frac{D_p^2 C_m \rho_p g}{18\mu} + \frac{3}{2} C_m \frac{R\mu}{MP} \frac{k}{2k + k_p} \frac{\Delta T}{x} . \quad (50)$$

Figure 11 is a plot of the data of Harrington and Crozier with lines obtained from Equation (50) included. These tests were made with a mixture of clay and a silica powder known by the commercial name of "Celite." For best results using Equation (49), it would be better to work with an average z rather than z_w , however, this was the value given.

In order to show the usefulness of thermal precipitation for the sampling of aerosols, Figure 12 is presented. This is a plot of the terminal settling velocity of water droplets in thermal and gravitational fields. The utility of thermal repulsion for sampling particles in the size range below 1×10^{-3} cm. is readily apparent.

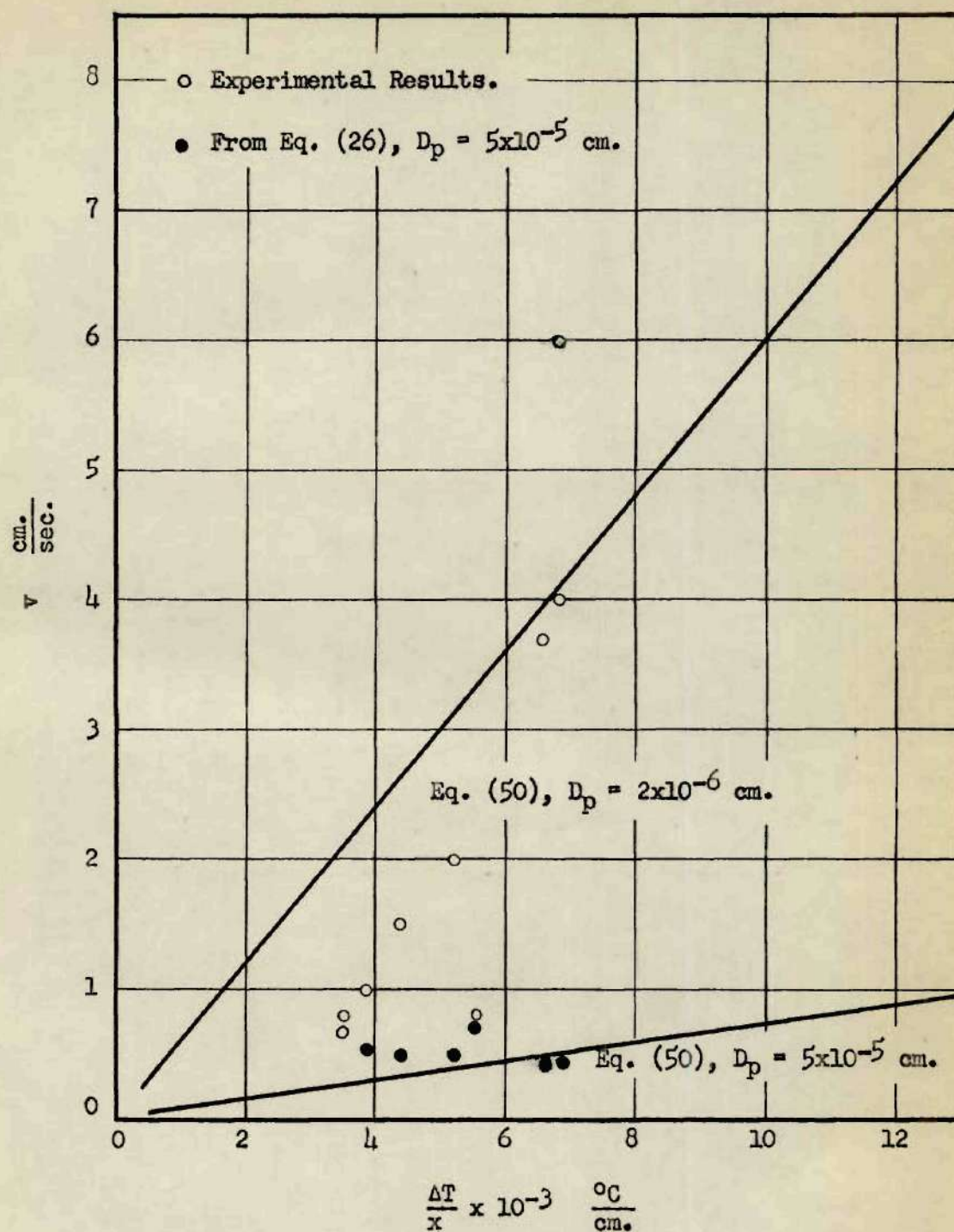


Figure 11. Results of Harrington and Crozier (14).

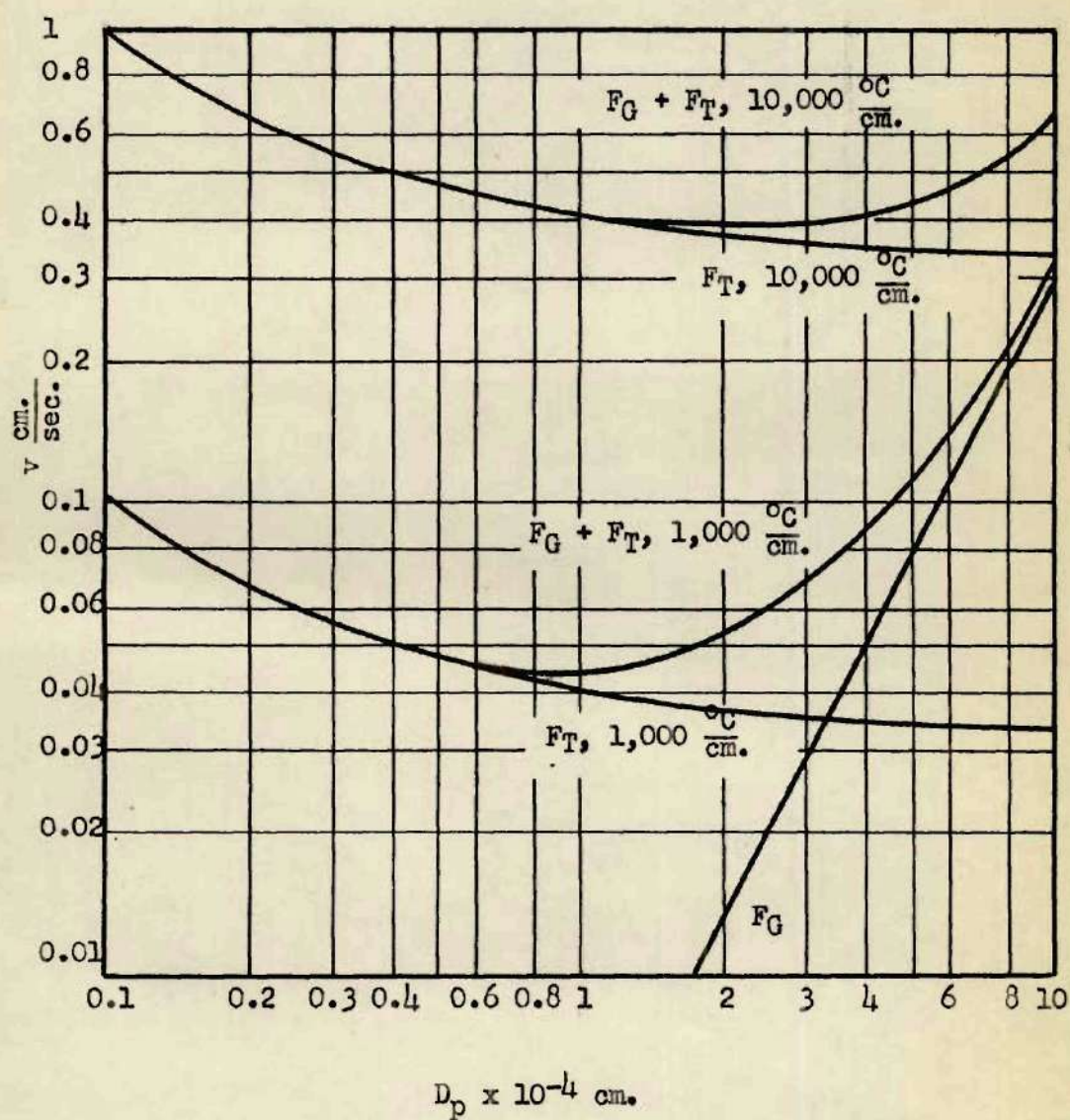


Figure 12. The Terminal Settling Velocity of Water Droplets in Thermal and Gravitational Fields.

CHAPTER IV

CONCLUSIONS

The following statements may be made as a result of this investigation of thermal precipitation and aerosol sampling:

1. The terminal velocity of an aerosol particle, moving in a thermal field only, may be expressed by the equation

$$v = \frac{3}{2} C_m \frac{R\mu}{MP} \frac{k}{2k + k_p} \frac{\Delta T}{x} .$$

2. The terminal velocity of an aerosol particle moving in a gravitational and thermal field acting in the same direction may be expressed by the equation

$$v = \frac{D_p^2 C_m \rho_p g}{18\mu} + \frac{3}{2} C_m \frac{R\mu}{MP} \frac{k}{2k + k_p} \frac{\Delta T}{x} .$$

A change in sign makes this equation applicable when the two fields are opposed.

3. A thermal precipitator has been developed and described which is being used for the routine sampling of all kinds of aerosols containing micron and sub-micron particles at flow rates considerably higher than those in thermal precipitators in common use.

4. Expressions for the terminal velocity of particles collected in areal-type thermal precipitators have been derived in terms of the

volume rate of flow of the sample, the deposit length and the inlet radius.

5. The thermal precipitators described herein can be used to deposit airborne bacteria for microscopic examination; however, a technique for the culture of the deposited bacteria has not been developed.

CHAPTER V

RECOMMENDATIONS

The results of experiments described herein confirm in a general way the equations presented. Further experimentation using mono-dispersed aerosols and a more precise method of measuring deposit lengths would serve to increase the utility of the equations developed.

The development of a method with which bacteria could either be removed from the glass cover slip and cultured or cultured directly on the glass cover slip is essential to the complete utilization of the areal-type thermal precipitator in microbiological studies.

An investigation of the use of thermal precipitation to separate different species of airborne particles on the basis of differences in thermal conductivity, would appear to be profitable. This might present a method for the separation and analysis of the various constituents of fumes and smokes.

A P P E N D I X

Sample Calculations

For Item No. 1, Table 10,

$$\frac{v}{U} = \frac{1}{\pi z (z + 2r_0)} ,$$

and if $\pi = 3.14$, $z = 0.39$ in., and $r_0 = 0.188$ in., then

$$\frac{v}{U} = 1.03 \text{ in.}^{-2} ,$$

or multiplying by $(1/2.54)^2$ gives

$$\frac{v}{U} = 0.16 \text{ cm.}^{-2} .$$

However, $U = 120 \text{ cm.}^3/\text{min.} = 2 \text{ cm.}^3/\text{sec.}$, or

$$v = 0.32 \text{ cm.}/\text{sec.} ,$$

and

$$\frac{\Delta T}{x} = \frac{43^\circ\text{C}}{(0.005 \text{ in.})(2.54 \text{ cm.}/\text{in.})} = 3390 \text{ }^\circ\text{C}/\text{cm.}$$

To obtain the line representing Equation (38) in Figure 7, the following substitutions were made:

$$D_p = 2 \times 10^{-6} \text{ cm.},$$

$$C_m = 11.01,$$

$$\rho_p = 0.8,$$

$$g = 980 \text{ cm.}/\text{sec.}^2,$$

$$\mu = 0.00019 \text{ poise},$$

$$\begin{aligned}
 R &= 82.06 \text{ cm}^3\text{-atm./gm.-mol. } ^\circ\text{K}, \\
 M &= 29, \\
 P &= 1 \text{ atm.}, \\
 k &= 0.066 \times 10^{-3} \text{ gm.-cal./cm.-sec.-}^\circ\text{C}, \\
 k_p &= 1.46 \times 10^{-3} \text{ gm.-cal./cm.-sec.-}^\circ\text{C}, \\
 \Delta T &= 100^\circ\text{C}, \text{ and} \\
 x &= 0.01 \text{ cm.}
 \end{aligned}$$

Thus,

$$v = 1 \times 10^{-8} + 3.69 \times 10^{-4} \frac{\Delta T}{x},$$

and the intercept, at $\frac{\Delta T}{x} = 0$, is approximately 1×10^{-8} cm./sec. When $\frac{\Delta T}{x} = 10,000$ $^\circ\text{C/cm.}$, $v = 3.69$ cm./sec.

The other theoretical lines were obtained in a similar manner.

For Figure 11, the value of v as a function of $\frac{\Delta T}{x}$ for the precipitators of Harrington and Crozier (14) was determined by substituting the values given in Table 14 with additional data from Table 3 on the properties of "Celite" into Equation (50). This gives

$$v = -0.106 \cdot 10^{-3} + 0.132 \cdot 10^{-3} \frac{\Delta T}{x},$$

for $D_p = 0.5 \times 10^{-4}$ cm. This line is plotted in Figure 11 along with values for other diameter particles.

Table 14. Experimental and Calculated Data from
Harrington and Crozier (14)

Item No.	Flow Rate	Area of Deposit	Temperature Difference	v^a	v^b	$\frac{\Delta T}{x}$
	U $\left(\frac{\text{cc.}}{\text{sec.}}\right)$		ΔT (°C)			
1	16.7	2.8	344	6.0	0.45	6880
2	16.7	4.2	341	4.0	0.42	6820
3	16.7	4.5	330	3.7	0.45	6600
4	8.3	4.2	261	2.0	0.50	5220
5	8.3	5.6	219	1.5	0.50	4380
6	8.3	8.5	194	1.0	0.54	3880
7	6.7	8.5	276	0.8	0.71	5520
8	3.3	4.2	175	0.8	0.68	3500

Constants: P = 0.84 atmospheres,

$\lambda = 1.2 \times 10^{-5}$ cm.,

$D_p = 0.5 \times 10^{-4}$ cm.,

$C_m = 1.4$,

$x = 0.05$ cm., and

$\mu = 0.00027$ poise.

^aFrom Equation (49).

^bFrom Equation (26).

Derivations

Equation (47) was derived in the following manner. From the geometry of the heated surface, it can be shown that

$$x = x_0 + \partial - \frac{\partial}{z_0} z ,$$

and that, therefore,

$$u = \frac{dz}{dt} = \frac{U}{2\pi \left[r_0 (x_0 + \partial) - \left(x_0 + \partial + \frac{r_0 \partial}{z_0} \right) z + \frac{\partial}{z_0} z^2 \right]} .$$

Separating variables and integrating between limits, it follows that

$$t = \frac{2\pi z}{U} \left[r_0 (x_0 + \partial) - \left(x_0 + \partial + \frac{r_0 \partial}{z_0} \right) \frac{z}{2} + \frac{\partial}{z_0} \frac{z^2}{3} \right] .$$

In this same time, t , the particle traverses the distance $(x_0 + \partial)$, or

$$t = \frac{x_0 + \partial}{v} .$$

Equating the above two equations gives

$$v = \frac{U (x_0 + \partial)}{2\pi z \left[r_0 (x_0 + \partial) - \left(x_0 + \partial - \frac{r_0 \partial}{z_0} \right) \frac{z}{2} + \frac{\partial}{z_0} \frac{z^2}{3} \right]} ,$$

which is Equation (47).

Equation (48) was derived in the following manner. From the

geometry of the heated surface, it can be shown that

$$x = x_0 + \partial - \frac{\partial}{z_0} z ,$$

and that, therefore,

$$u = \frac{dz}{dt} = \frac{U}{2\pi \left[r_0 (x_0 + \partial) + \left(x_0 + \partial - \frac{r_0 \partial}{z_0} \right) z - \frac{\partial}{z_0} z^2 \right]} .$$

Separating variables and integrating between limits, it follows that

$$t = \frac{2\pi z}{U} \left[r_0 (x_0 + \partial) + \left(x_0 + \partial - \frac{r_0 \partial}{z_0} \right) \frac{z}{2} - \frac{\partial}{z_0} \frac{z^2}{3} \right] .$$

In this same time, t , the particle traverses the distance $(x_0 + \partial)$, or

$$t = \frac{x_0 + \partial}{v} .$$

Equating the above two equations gives

$$v = \frac{U (x_0 + \partial)}{2\pi z \left[r_0 (x_0 + \partial) + \left(x_0 + \partial - \frac{r_0 \partial}{z_0} \right) \frac{z}{2} - \frac{\partial}{z_0} \frac{z^2}{3} \right]} ,$$

which is Equation (48).

Calculation of Spacing

With thermal precipitators Models I and II, the thermal gradient varied with z due to the sloping hot surfaces. An arithmetic average of the gradient was used. This average was obtained by dividing the temperature difference by the average spacing as determined from the expression

$$x_{ave.} = x_0 + \partial - \frac{\partial}{z_0} \frac{z}{2} \quad .$$

Assembly and Operating Instructions for
Thermal Precipitators, Models II and IIA

1. Attach water lines to the cold plate.
2. Place the insulating spacer on the cold plate over the four studs. The spacer surfaces should be greased to ensure air-tightness.
3. Place a glass cover slip, celluloid disk, or other substrate in the cavity in the cold plate. The cavity should be moistened with several drops of water to maintain good thermal contact and to ensure that the cover slip or disk remains in place.
4. Place the hot plate on the insulating spacer over the four studs and complete the assembly by fastening the wing-nuts.
5. Start the cooling water and attach the heater to a continuously variable autotransformer. Care should be taken not to heat the unit until the apparatus is assembled and the cooling water running.
6. Wait fifteen minutes for the hot plate to attain proper temperature and then start sampling.
7. Adjust the sampling rate to the desired value with a suitable flow meter.
8. After sampling for the desired length of time, switch off the current and disassemble the device to obtain the deposited sample.

Symbols¹.

Latin Letter Symbols

- A Constant in Cunningham's correction factor to Stokes' Law = 0.86 Dalla Valle (8)
- B Constant in Watson's (25) equation
- C_m Cunningham's correction factor to Stokes' Law = $1 + \frac{2A\lambda}{D_p}$
- C Average molecular velocity
- D_p Particle diameter
- E Figure of merit used by Harrington and Crozier (14)
- F Force
- f Heat or energy flow per unit area
- g Acceleration of gravity
- k Gas thermal conductivity
- k_p Particle thermal conductivity
- M Molecular weight of gas
- m Mass of gas molecules
- N Number of molecules
- n Avogadro's number
- P Absolute pressure
- Q Heat flow per unit time per unit area
- R Gas constant
- r Radius
- r_o Inlet radius of areal thermal precipitator

¹Except where noted in the text, any self-consistent system of units may be used.

- T Absolute temperature
 ΔT Temperature difference
 t Time
 U Volume rate of flow of gas
 u Velocity of gas
 v Particle terminal velocity
 w Width
 x Distance between hot and cold surface; dark space thickness
 x_0 Distance between parallel parts of the hot and cold surfaces of areal thermal precipitator
 z Length of deposit in areal-type precipitator = radius of deposit - radius of inlet opening
 z_0 Length of sloped portion of hot plate

Greek Letter Symbols

- α Exponent in Watson's (25) equation
 Δ Finite difference
 ∂ The elevation of the extreme edge of the hot surface above the flat section
 μ Gas viscosity
 ρ Density of gas
 ρ_p Density of particle

Latin Letter Subscripts

- a Gas phase
 G Gravitational
 o Limiting value of a variable

p Particle
T Thermal
V Viscous drag

Abbreviations

atm. Atmospheres
ave. Average
°C Degrees Centigrade
cal. Calorie
cc. Cubic centimeters
cm. Centimeters
°F Degrees Fahrenheit
gm. Grams
in. Inch
°K Degrees Kelvin
micron 10^{-4} centimeters
min. Minute
mol. Molecular weight
No. Number
sec. Second

BIBLIOGRAPHY

1. Aitken, J., "On Formation of Small Clear Spaces in Dusty Air." Philosophical Transactions of the Royal Society of Edinburgh 32, 239 (1884).
2. Bancroft, W. D., "Thermal Filters." The Journal of Physical Chemistry 24, 421 (1920).
3. Betz, J. D., and Noll, C. A., "Total Hardness Determination by Direct Colorimetric Titration." Journal of the American Water Works Association 42, 49 - 56 (1950).
4. Blacktin, S. C., "The Cleaning of Air and Gas by Thermal Repulsion." Journal of the Society of Chemical Industry (London) 88, Pt. 2, 334 (1939).
5. Bredl, J., and Grieve, T. W., "A Thermal Precipitator for Gravi-metric Estimation of Solid Particles in Flue Gases." Journal of Scientific Instruments 28, 21 (1951).
6. Cawood, W., "The Movement of Dust or Smoke Particles in a Temperature Gradient." Transactions of the Faraday Society 32, 1068 (1936).
7. Crookes, W., "On Repulsion from Radiation." Philosophical Transactions of the Royal Society (London) 170-1, 87 (1879).
8. Dalla Valle, J. M., Micromeritics, Pitman Publishing Company, New York, 1948.
9. Diehl, H., Goetz, C. A., and Hach, C. C., "The Versenate Titration for Total Hardness." Journal of the American Water Works Association 42, 40 - 48 (1950).
10. Einstein, A., "Zur Theorie der Radiometerkrafte." Zeitschrift für Physik 27, 1 (1924).
11. Epstein, P., "Zur Theorie der Radiometers." Zeitschrift für Physik 54, 537 (1929).
12. Gordon, M. T., "Thermal Repulsion." The Research Engineer 7, 9 (1953).

13. Gordon, M. T., and Orr, Clyde, Jr., Thermal Precipitation in Air Pollution Studies. Presented at the Annual Meeting of the Air Pollution Control Association, Chattanooga, Tennessee, May 2 - 5, 1954.
14. Harrington, E. R., and Crozier, W. D., A Thermal Precipitator for Sparse Dispersions of Aerosols. Technical Report No. 2-NR, Contract N7ONR-405, New Mexico School of Mines, Research and Development Division, 1948.
15. Jakob, Max, Heat Transfer, Vol. I, John Wiley and Sons, Inc., New York, 1949.
16. Kethley, T. W., Gordon, M. T., and Orr, C., Jr., "A Thermal Precipitator for Aerobacteriology." Science 116, 368 (1952).
17. Knudsen, M., "Eine Revision der Gleichgewichtsbedingung der Gase Thermische Molekulantromung." Annalen der Physik 31, 205 (1910).
18. Maxwell, J. C., "On stresses in Rarified Gases Arising from Inequalities of Temperature." Philosophical Transactions of the Royal Society (London) 170, 231 (1879).
19. Perry, J. H., ed. Chemical Engineers Handbook, 3rd ed., McGraw-Hill Book Co., Inc., New York, 1950.
20. Rayleigh, Lord, "On the Dark Plane Which is Formed Over a Heated Wire in Dusty Air." Proceeding of the Royal Society (London) 34, 414 (1882).
21. Reynolds, O., "On Forces Caused by Communication of Heat Between a Surface and a Gas." Philosophical Transactions of the Royal Society (London) 166, 725 (1876).
22. Rosenblatt, P., and Lamer, V. K., "Motion of a Particle in a Temperature Gradient; Thermal Repulsion as a Radiometer Phenomenon." The Physical Review 70, 385 (1946).
23. Saxton, R. L., and Ranz, W. E., "Thermal Force on an Aerosol Particle in a Temperature Gradient." Journal of Applied Physics 23, 917 (1952).
24. Tyndall, J., "On Dust and Disease." Proceedings of the Royal Institution of Great Britain 6, 3 (1870).
25. Watson, H. H., "The Dust-free Space Surrounding Hot Bodies." Transactions of the Faraday Society 32, 1073 (1936).